Conserving Nature's Stage: Mapping Omnidirectional Connectivity for Resilient Terrestrial Landscapes in the Pacific Northwest

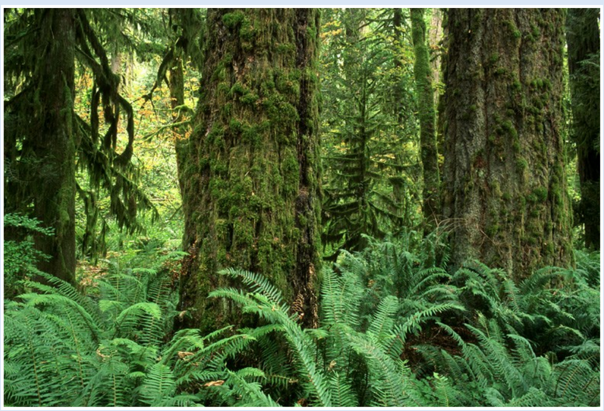

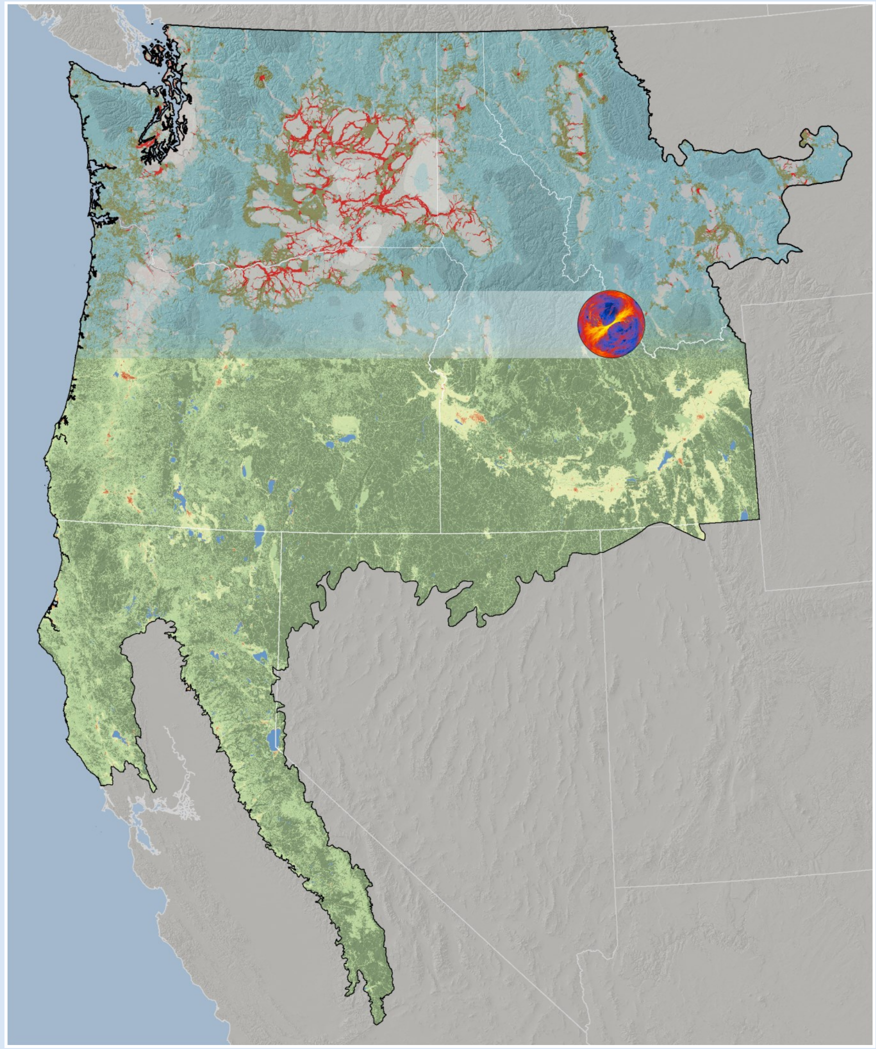

Pacific Northwest and Northern California
Final Report
to the Doris Duke Charitable Foundation
June 2016

Brad McRae
Ken Popper
Aaron Jones
Michael Schindel
Steve Buttrick
Kimberly Hall
Bob Unnasch
Jim Platt

The Nature Conservancy

Cover Photo Credits:
Top photo- Oak savanna, Willamette Valley ©Rick McEwan
Second photo- Sandy River old growth ©Harold E. Malde
Third photo- Zumwalt Prairie ©Michael Durham
Bottom photo- Boardman Grassland ©Rick McEwan

Please cite as: McRae, B.H., K. Popper, A. Jones, M. Schindel, S. Buttrick, K. Hall, R.S. Unnasch, and J. Platt. 2016. Conserving Nature's Stage: Mapping Omnidirectional Connectivity for Resilient Terrestrial Landscapes in the Pacific Northwest. The Nature Conservancy, Portland Oregon. 47 pp. Available online at: http://nature.org/resilienceNW June 30, 2016.

Table of Contents

Acknowledgements

We thank the Doris Duke Charitable Foundation whose generous grants to The Nature Conservancy made this work possible. We also thank the Wilburforce Foundation for supporting development of the OmniScape methods and code, which were considerably improved through a collaborative project with The Nature Conservancy's California Chapter. We also thank those who provided input on our modeling methods, feedback on this report, and counsel on applied conservation needs including Mark Anderson, Dick Cameron, Carlos Carroll, Melissa Clark, Joe Fargione, Josh Lawler, Caitlin Littlefield, Catherine Macdonald, Julia Michalak, Carrie Schloss, and David Theobald. Thanks to Dani O'Brien for her formatting and production of the final documents.

Project History, Scope, and Setting

This report completes a larger project to identify and map sites that contribute to climate change resilience in the Pacific Northwest, all funded by the Doris Duke Charitable Foundation. Previous work (reported in Buttrick et al. 2015) focused on mapping sites likely to be resilient to climate change based on local permeability and topoclimate diversity. Those sites that were more locally intact and topoclimatically diverse were considered more resilient to climate change because they would have higher potential to allow organisms to access climatically suitable areas by moving short distances. The previous analyses purposefully considered the local scale, not looking beyond a 3-km window when measuring terrestrial resilience characteristics. Results were stratified by ecoregion and by geophysical setting ("land facets") to identify portions of land facets more likely to be resilient to climate change.

The broad-scale landscape connectivity analysis reported here complements these previous analyses by identifying areas likely to facilitate ecological flow—particularly movement, dispersal, gene flow, and distributional range shifts for terrestrial plants and animals—over large distances and long time periods. Similar to the local permeability analyses (Buttrick et al. 2015), this analysis is not species-specific. Rather, it focuses on structural connectivity of natural lands, with *resistance* to movement modeled as a function of landscape naturalness. This analysis shifts the focus to identifying areas important for longer-distance movements – up to 50 km – complementing the local permeability analyses which identified areas well-connected within a 3-km radius. This effort does not incorporate projections of future climates, nor does it address connectivity for aquatic species. The results identify broad, intact areas where movement of terrestrial organisms is largely unrestricted by human modifications to the landscape, as well as constricted areas where fragmentation has reduced movement options and further habitat loss could isolate remaining natural lands. We provide guidance on how these results can be combined with the resilient sites analyses of Buttrick et al. (2015), as well as other conservation priorities.

Our project area covers 97.3 million hectares (240.4 million acres) of the Pacific Northwest and northern California. This includes 92 million hectares (227 million acres) analyzed in Buttrick et al. (2015) — namely, the California North Coast, Klamath Mountains, Sierra Nevada, West Cascades, East Cascades/Modoc Plateau, Columbia Plateau, and Middle Rockies/Blue Mountains ecoregions as well as the U.S. portion of the Pacific Northwest Coast, Willamette Valley/Puget Trough, North Cascades and Canadian Rockies ecoregions. This connectivity study also encompasses an additional 5.3 million hectares (13.4 million acres) comprising the U.S extent of the Okanagan ecoregion and the extent within Idaho of the Utah-Wyoming Rocky Mountains ecoregion (Map 1).

Map 1: Study Area / Figure Index

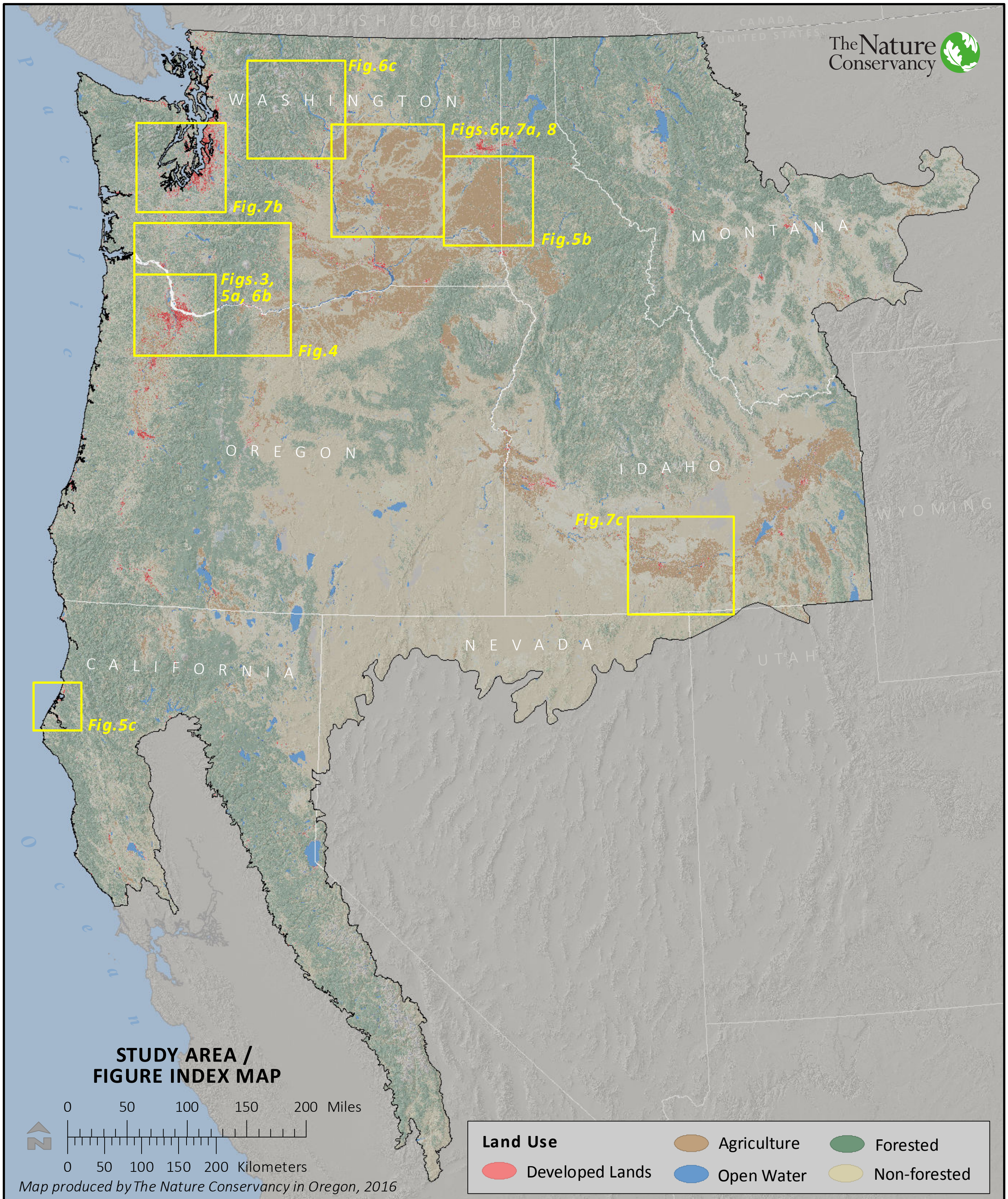

The geographic extents of report figures are indicated in this map to help orient the reader. Generalized land use/land cover data are also shown for reference. Total project area was 97.3 million hectares, including all or part of 13 ecoregions.

Introduction

Landscape connectivity and Conserving Nature's Stage

The "Conserving Nature's Stage" strategy focuses on identifying places that are likely to be good conservation investments now and under future climate change. Maintaining landscape connectivity is a key part of the Conserving Nature's Stage approach (Anderson et al. 2012, 2014, Beier et al. 2015). One of the most important ways species have responded to past climatic changes has been to shift their ranges to track suitable climates (Jackson et al. 2000, Krosby et al. 2010, Blois et al. 2013, Moritz et al. 2013, Gill et al. 2015) Rapid warming projected for the next century will likely require many species and populations to adapt in similar ways or face extinction (Thuiller et al. 2005, Lawler et al. 2013). Many species are already moving in response to rapid warming (Chen et al. 2011).

Increased high levels of anthropogenic habitat loss and fragmentation mean that many species will likely encounter barriers that weren't present during past periods of climate change (Warren et al. 2001, Thomas et al. 2010, Corlett and Westcott 2013, Gill et al. 2015). This, combined with rapid climate change projected for the coming century, means that many species may not be able to move quickly enough or far enough to keep up as suitable climates shift across the landscape (Loarie et al. 2009, Schloss et al. 2012, Lawler et al. 2013). Moreover, maintaining gene flow and genetic diversity through dispersal will be increasingly important for species adapting to climate change *in situ* (Hoffmann & Sgrò 2011, Sexton et al. 2011, Sgrò et al. 2011). For these and other reasons, conserving connectivity is the most recommended strategy for conserving biodiversity under climate change (Heller and Zavaleta 2009).

Mapping connectivity at multiple scales

As with climate resilience analyses in the eastern USA (Anderson et al. 2012), we have identified a need to map areas that contribute to the ability of species to adapt to climate change through both local and long-distance movements. The previously completed **local terrestrial permeability** analysis for this study area (Buttrick et al. 2015) quantified local connectedness of the immediate neighborhood surrounding every pixel in the study area, measuring connectedness of that pixel to its neighborhood out to a maximum distance of 3 km. By doing so, that analysis estimated the ability of species to move short distances in order to find suitable habitats or microclimates under climate change. The **broad-scale connectivity** analysis described in this report complements the local connectedness analysis by modeling the potential for movements among natural lands separated by distances up to 50 km. It estimates how flow patterns at this scale may become diminished, redirected, or concentrated through certain areas due to the spatial arrangements of cities, towns, farms, roads, open water, and natural land.

Our definition of connectivity (modified from Meiklejohn et al. 2010) is: *the degree to which regional landscapes, encompassing a variety of natural, semi-natural and developed land cover* *types, will sustain ecological processes and are conducive to the movement of many types of organisms.* Thus, we focus on areas that will be important for facilitating the local- and regional-scale terrestrial ecological reorganization expected from climate change, involving many types of organisms, over long time periods, among all types of natural and semi-natural habitats. Our assumption is that maintaining a connected landscape, in conjunction with protecting and restoring sufficient areas of high-quality habitat, will facilitate climate-induced range shifts and community reorganization.

Species respond individualistically to climate change, and do not always move upslope or poleward to cooler areas; instead, some have moved downslope in response to gradients in water availability and other climate variables (Jackson and Overpeck 2000, Crimmins et al. 2011, Rapacciuolo et al. 2014, Gill et al. 2015). Thus our primary analysis represents a coarse-filter approach (Noss 1987) that sought to quantify the existing structural connectivity of natural lands with no consideration of predicted changes in temperature, precipitation, or other climate variables. Avoiding explicit projections of how the climate will change was also in keeping with the Conserving Nature's Stage approach, which seeks to identify sites likely to contribute to climate resilience in a way that is robust to uncertainties about how climate change will play out on the landscape (Anderson et al. 2012, 2014, Beier et al. 2015, Buttrick et al. 2015, Lawler et al. 2015). However, we also include a pilot analysis that connects across climate gradients – from warm to cool areas – to demonstrate the flexibility of our methods and their applicability with additional climate data.

Both the local and broad-scale models are based on measures of human modification to the landscape, with natural lands presenting the least resistance to movement, and developed lands and human-created barriers such as highways causing the most resistance to movement. Although both analyses focused on natural and semi-natural lands, we recognize that species respond differently to anthropogenic land use, and that in fact there are species that thrive in heavily-modified landscapes. Such species were not the target of this analysis. Connectivity for aquatic species was also not addressed. Rather, this report identifies areas important for maintaining connectivity for terrestrial species dependent on natural landscapes for movement, survival, and reproduction.

Modeling broad-scale connectivity: a new approach

We used Circuitscape (McRae et al. 2013a; http://www.circuitscape.org/) with a novel moving-window analysis to quantify flow among all natural and semi-natural lands up to a distance of 50 km. Circuitscape models connectivity using electric circuit theory and leveraging mathematical connections between circuit and random walk theories. It incorporates all possible pathways between movement sources and destinations and identifies movement via low-resistance routes, i.e., routes presenting relatively low movement difficulty and mortality risk. Circuitscape works by treating landscapes as resistive surfaces, where high-quality movement habitat has low resistance and barriers have high resistance. When two features on the landscape are to be connected, electrical current flows from one (the source) to the other (the target). Patterns of current flow through intervening areas help identify important routes for movement.

Previous applications have shown that three basic patterns can be seen in the products produced by Circuitscape. Current flow will 1) avoid (be *impeded* by) areas with strong movement barriers, 2) concentrate (*intensify*) in key linkages where flow accumulates or is *channeled* through *pinch-points* (bottlenecks), and 3) spread out (*diffuse*) in highly intact areas with few barriers (Anderson et al. 2012). A primary use of Circuitscape has been to identify high-flow areas, particularly pinch-points, where the loss of a small amount of movement habitat could disproportionately compromise connectivity (e.g., Dickson et al. 2013).

Traditional applications of Circuitscape for conservation planning have typically focused on connecting pairs of core areas or patches (e.g., Dickson et al. 2013, Brodie et al. 2015, Vasudev and Fletcher 2015). This requires breaking the landscape into discrete core areas to be connected and matrix lands between them.

Our development of the moving window approach was inspired by recent efforts that have used Circuitscape to create ‘wall-to-wall’ connectivity maps, particularly Anderson et al. (2012, 2014), Koen et al. (2014), and Pelletier et al. (2014). These methods modeled electrical current passing through a given region as it flowed between sources and destinations placed in buffer areas surrounding the region. For example, the wall-to-wall method employed by Anderson et al. (2012, 2014) and Pelletier et al. (2014) used a tiling approach, in which a landscape is broken down into square tiles surrounded by a buffer area, and current is passed across each tile from a source beyond one edge of the tile to a ground beyond the opposite edge (Fig. 1). This is repeated for each of the four cardinal directions and the four current maps are summed. Tiles are then reassembled to create continuous, omnidirectional connectivity maps. The resulting mosaics highlight pinch-points, where movement appears to be channeled through the landscape.

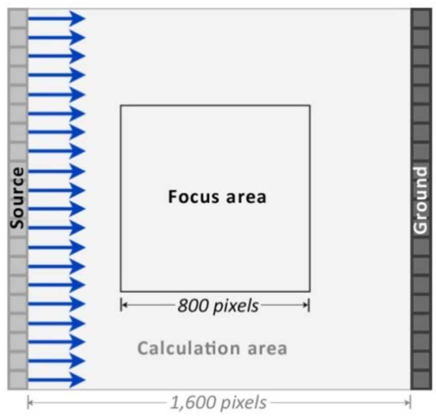

Figure 1. 'Wall-to-wall' Circuitscape method, in which current typically flows across each tile in each of the four cardinal directions (in this case from West to East) with the four results summed to produce a single current map. Buffer areas are then removed and tiles are stitched together. Adapted from Anderson et al. (2012).

This approach represented a significant advance because it created seamless maps of broad-scale connectivity without the need to divide the landscape into a binary representation of matrix lands and core areas to be connected. This is important because arbitrary decisions about how core areas are defined, e.g., minimum size requirements, can strongly influence connectivity modeling results (Carroll et al. 2010, Koen et al. 2014, Pelletier et al. 2014). Identifying core areas to connect can be desirable in some cases, e.g., when discrete animal populations are well mapped or when the goal is to connect existing protected areas in a network (e.g., Brodie et al. 2015, Dutta et al. 2015). Delineating areas to connect can be problematic, however, in studies such as ours where the goal is to model connectivity for different kinds of processes across a large region; the approach can also obscure important connectivity routes within core areas.

We built on the wall-to-wall methods in a way that retained the ability to map connectivity without the need to delineate discrete core areas, but still allowed us to define what types of lands were connected to one another, how strongly they were connected, and over what distances. In other words, even with continuously-mapped landscape features we wanted to:

- explicitly connect those features (e.g., natural areas) that represented important conservation targets for those using our products;
- adjust flow depending on site characteristics, e.g., allowing more flow to emanate from—and travel to—lands in more natural condition;
- map flow only between areas close enough to one another to be connected for most movement processes within realistic planning horizons and planning scales.

Thus our method built on previous efforts by adding the capacity to define which features were to be connected while still maintaining a continuous, "core-free" connectivity modeling approach.

Being explicit about what is to be connected has several advantages. It recognizes that sources and destinations for movement are essential to the concept of connectivity, and that some areas are more important to connect than others. Moreover, the ability to specify what is being connected is critical for any future efforts to use our method to model connectivity across climate gradients. For example, applications that focus on identifying pathways that connect warm areas to cooler areas (as in Nuñez et al. 2013, McGuire et al. 2016) or connect sites that have a specific set of climate conditions to sites projected to have those climate conditions in the future (as in Littlefield et al. in review) require that source-target pairs be explicitly defined.

The Omnidirectional Circuitscape (OmniScape) algorithm

We developed an algorithm that modeled connectivity between natural and semi-natural areas using a circular moving window. We prioritized connecting pixels representing natural lands, reflecting our assumption that these areas were the most important to connect. We also connected semi-natural areas, such as agricultural lands and urban open spaces, but adjusted the flow originating from and arriving at such areas based on their level of human modification. In other words, natural areas generated and received more flow than semi-natural areas, and these in turn generated and received more flow than heavily-modified areas.

Following the work of Nuñez et al. (2013), which also sought to identify areas important for connectivity under climate change, we chose to connect natural and semi-natural lands within 50 km of one another. This balanced the desire to examine broad-scale connectivity with computational tractability, but also focused our analyses on movements that fall within realistic conservation planning scales and time horizons.

The algorithm required first defining what types of land uses were to be connected, and assigning resistances to different landscape features. It then used a moving window to connect all pixels within the 50-km radius to one another using Circuitscape, summing up results from each moving window into a cumulative current map. We describe the method and resulting maps in detail below.

Resistance and source weight modeling

As in other applications of Circuitscape, the algorithm we developed represents a landscape as a resistive surface. Landscape features conducive to movement are given low resistances, and features that act as barriers to movement are given higher resistances.

We created a resistance raster surface at 180 m resolution using a process and input data similar to those used for resistance modeling to support the local landscape permeability analyses reported by Buttrick et al. (2015). This involved combining data on land use, roads, energy infrastructure, housing density, and other features. Details about this process are in Appendix A. The resulting resistance raster is shown in Map 2.

In addition to variability in resistance to movement, we also assumed that landscape features vary in their importance for being connected. For example, natural areas may provide better habitat for native species and therefore act as more important sources and destinations for movement. Connecting such areas is likely to be of greater importance to conservation managers than connecting non-natural areas. To represent the variation in importance for connecting different areas, we created a surface of *source weights* which reflect the differing value we place on

Map 2: Terrestrial Resistance

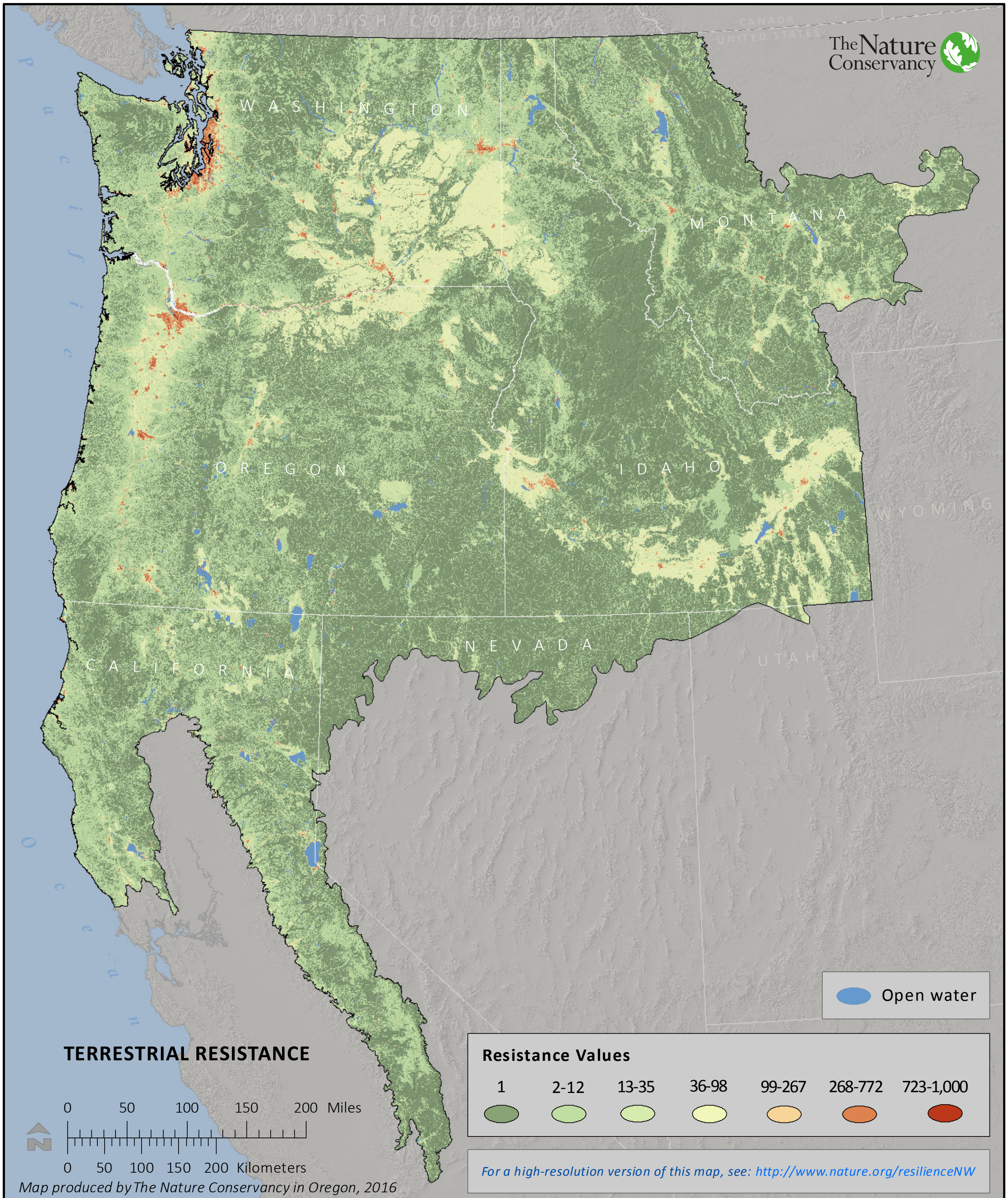

This map shows resistance to movement, the first of two datasets which underpin our regional connectivity analysis. We modeled resistance based on the degree of human modification to the landscape, with low resistance values assigned to natural lands and high values assigned to developed lands, open water, and human-created barriers such as highways.

connecting different types of landscape features, with more natural pixels having higher source weights.

We used the same input data layers and a similar procedure to create a source weight raster as we did to create the resistance raster, in this case assigning greater source weights to land uses we considered more likely to support natural populations now or in the future, resulting in more flow to and from them. For example, areas consisting of entirely natural vegetation were given the maximum source weight of 1, whereas semi-natural areas were given lower source weights. Open water and completely developed areas were assigned a source weight of zero. The resulting source-weight raster, also created at 180 m resolution, is shown in Map 3.

The resistance and source weight rasters formed the inputs for subsequent analyses, with higher current flow occurring between areas with high source weights and along paths of low resistance. More detail about our resistance and source-weight modeling can be found in Appendix A. A table with resistance and source-weight scores for different land cover/land use classes is in Appendix B.

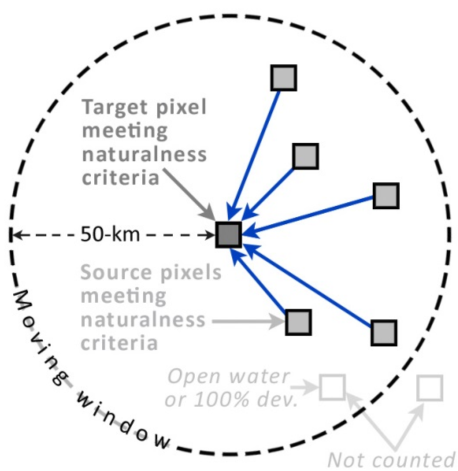

Figure 2. Illustration of the moving window method. In the simplest case, a moving window is passed over the resistance and source weight rasters, centering in turn on each pixel. If the center pixel meets the naturalness criteria for being a destination for movement, it is treated as a target for movement. All pixels within the moving window radius that meet the same criteria are considered sources. Current flows from all source pixels to the target pixel, with more current flowing from more natural source pixels.

Moving window algorithm

Once resistance and source weights were mapped, our algorithm modeled connectivity between pixels with non-zero source weights using a 50-km circular moving window. In the simplest formulation of the algorithm, the moving window passes over the resistance and source weight rasters described above, centering in turn on each pixel (Fig. 2). If the center pixel is not open water or completely developed, it meets the criteria for being a destination for movement. If these criteria are not met, i.e., the target pixel has a source weight of zero, the window moves on to the next target pixel without performing any calculations. All pixels within the moving window radius that meet these criteria are considered sources, but they can have different weights. Calculations are performed only for the moving window area; prior to calculating flow, the algorithm masks out all areas of the resistance layer that are outside of the 50-km circle. Masking increases computational efficiency while also limiting movements to no greater than 50 km from

Map 3: Source Weight

This map depicts source weights, the second dataset underpinning our regional connectivity analysis. Source weights were derived from similar input data layers and procedures as the resistance values, with greater source weights assigned to pixels in more natural condition. We modeled connectivity between all pixels with non-zero source weights (i.e., excluding only completely developed lands and open water), with higher current flow occurring between areas with high source weights.

the target. Once the area of analysis is defined, the algorithm calls Circuitscape. Circuitscape injects current from each source pixel, with more current flowing from more natural pixels. The target pixel is set to ground, so that current flows across the subsetted landscape from sources to the center target.

Note that each pixel that meets the criteria for being a source/target will be a source for many moving window iterations (i.e., as many as there are sources within 50 km), and a target for one iteration. Note also that in this model, barriers do not absorb or “kill” current; instead, they only re-route current. Current will take the best route possible, “punching through” barriers if needed.

The result is a current map for each target pixel showing areas important for connecting the source pixels within 50 km to the target pixel (Fig. 3). The moving window then shifts one pixel to the right, centering on the next target pixel; if that pixel meets the naturalness criteria (i.e., it is not entirely developed and is not open water), all other pixels meeting the criteria in the radius will be connected to it, and so on. Current maps are summed across all moving windows to create a cumulative current flow map among all sources and targets (Fig. 4).

Using blocks of target pixels as a computational shortcut

In practice, our method proved computationally prohibitive when calculations had to be repeated with the moving window centered on each and every natural or semi-natural pixel in the study region. To speed up processing, we employed a computational shortcut in which the moving window centered on square blocks of pixels rather than on each individual pixel. Each computation solved for all targets in a block; in this way, a single computation replaced many individual computations, speeding up the algorithm without lowering the resolution of the resistance data. More detail on this method can be found in Appendix C.

Mapping current flow across the study area

We used the above methods to produce a *current flow* surface for the study area, indicating where concentrations of natural land and barriers interacted to produce differing patterns of flow (Map 4).

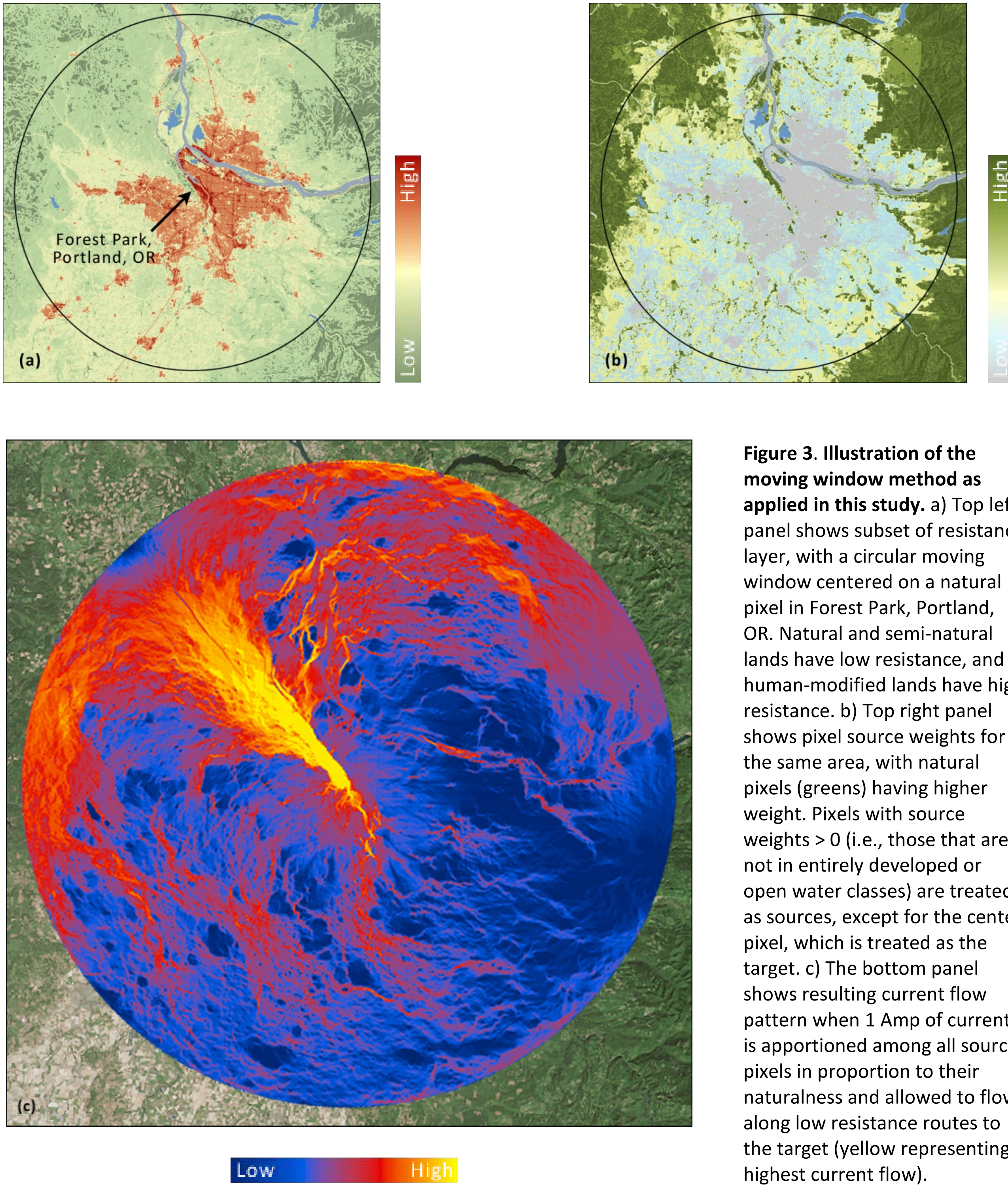

Figure 3. **Illustration of the moving window method as applied in this study.** a) Top left panel shows subset of resistance layer, with a circular moving window centered on a natural pixel in Forest Park, Portland, OR. Natural and semi-natural lands have low resistance, and human-modified lands have high resistance. b) Top right panel shows pixel source weights for the same area, with natural pixels (greens) having higher weight. Pixels with source weights > 0 (i.e., those that are not in entirely developed or open water classes) are treated as sources, except for the center pixel, which is treated as the target. c) The bottom panel shows resulting current flow pattern when 1 Amp of current is apportioned among all source pixels in proportion to their naturalness and allowed to flow along low resistance routes to the target (yellow representing highest current flow).

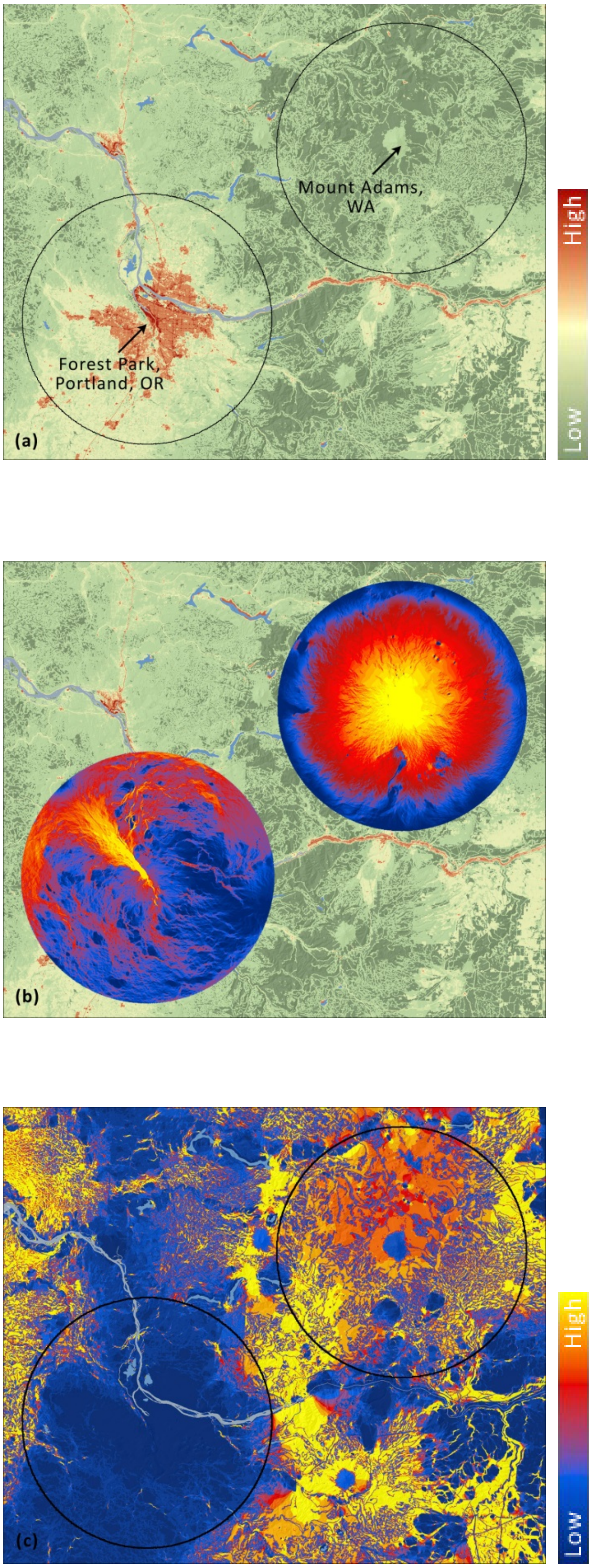

Figure 4. Summing individual moving window results to create a seamless current flow map. Top two panels show a) locations and b) results for two 50-km-radius moving windows (centered on the Portland, OR area and the less-human-modified area around Mount Adams, WA). In both windows, current concentrates toward the center of the window. But flow is less constrained – and thus more evenly spread – throughout the Mount Adams area. c) Bottom panel shows the same subset of the study area, with summed current flow from moving windows passed over the entire study area. Flow is lower in heavily modified areas like Portland because: 1) high resistance causes flow to divert around them when other routes are available; and 2) there are fewer natural areas to connect within 50 km, and thus current sources and targets are fewer and weaker.

In these raw current flow results, the patterns typically produced by Circuitscape are evident, with current avoiding areas with strong movement barriers, concentrating where flow is channeled through pinch-points, and diffusing in highly intact/highly permeable areas. Large urban centers often have low scores, both because flow is diverted around these areas by anthropogenic barriers and because naturalness scores tend to be low, on average, within 50 km of these centers (e.g., Portland; Fig. 5a). Flow can also be low in large agricultural areas with little natural land, e.g., the Palouse Prairie area south of Spokane, WA (Fig. 5b), or areas along the outer coast, even with relatively intact landscapes (Fig. 5c).

Areas with highest current flow tend to be those where natural or artificial barriers channel and concentrate flow. This is particularly evident in agricultural areas where linear stretches of natural land form corridors conducive to movement, e.g., in the northern portion of the Columbia Plateau Ecoregion in Washington (Fig. 6a). Similarly, natural, linear features that are surrounded by development form conduits, concentrating flow (e.g., Forest Park in Fig. 6b).

Map 4: Current Flow

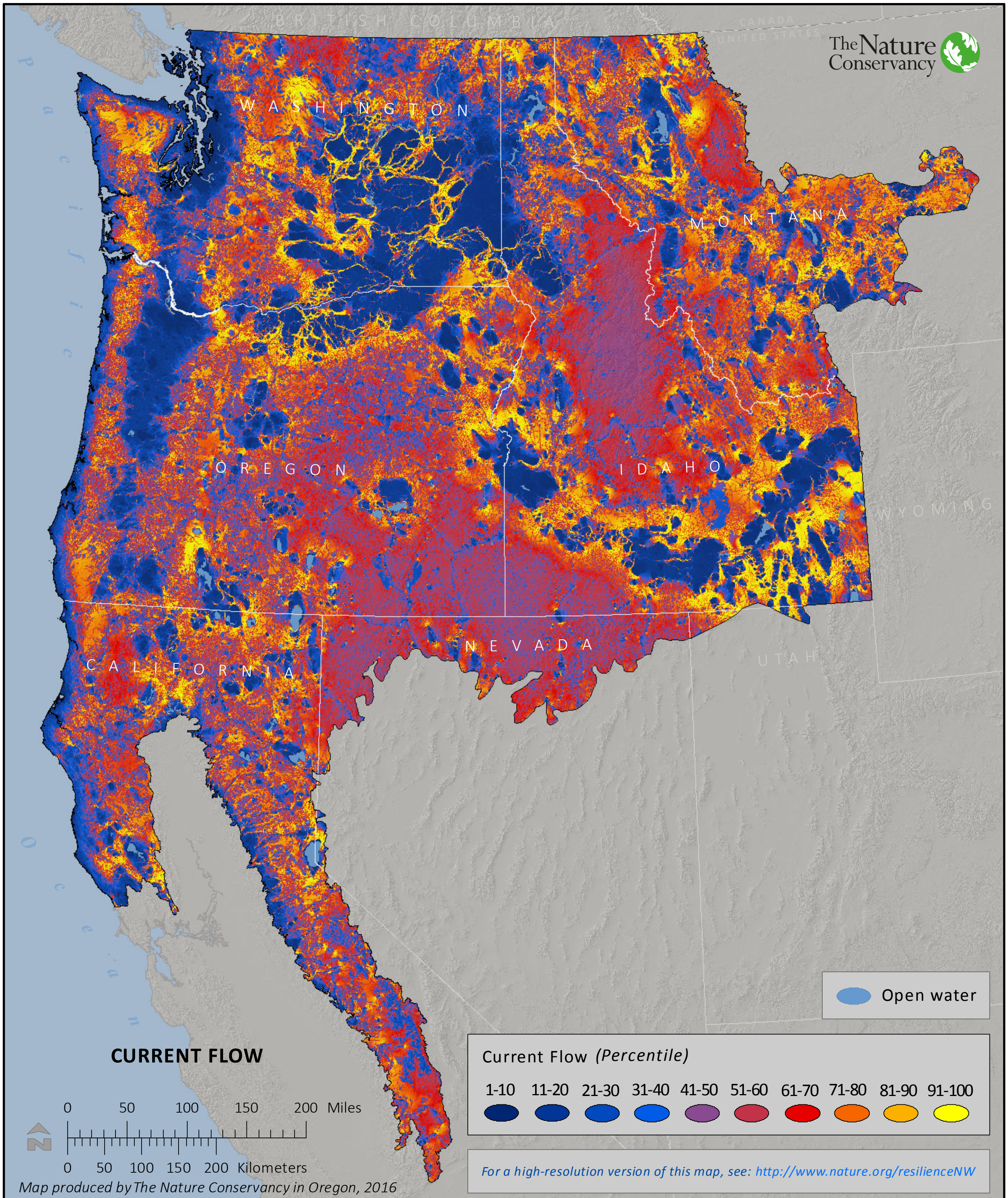

This map shows current flow for terrestrial connectivity among all natural and semi-natural pixels within 50 km of one another, created using the OmniScape moving window algorithm. The algorithm is illustrated in Figs. 2-4. Current flow is highest between areas with high source weights and along paths of low resistance.

Flow is also channeled around natural barriers. For example, Lake Chelan separates highly natural lands to the east and west (Fig. 6c). Moving windows that straddle but also include land to the north of the lake produce flow between eastern and western sides of the lake via the northern tip of the lake.

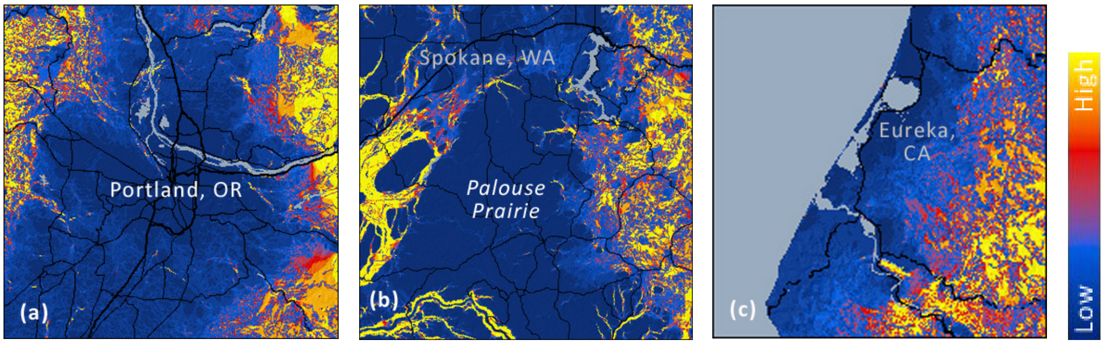

Figure 5. Example cases in which landscape configuration results in low current flow. Areas that have relatively few natural lands to connect and many barriers to movement include: a) urban areas such as Portland, OR; and b) intensive agricultural areas such as the Palouse Prairie. c) Areas along the outer coast tend to have low flow because they are not situated between large natural areas.

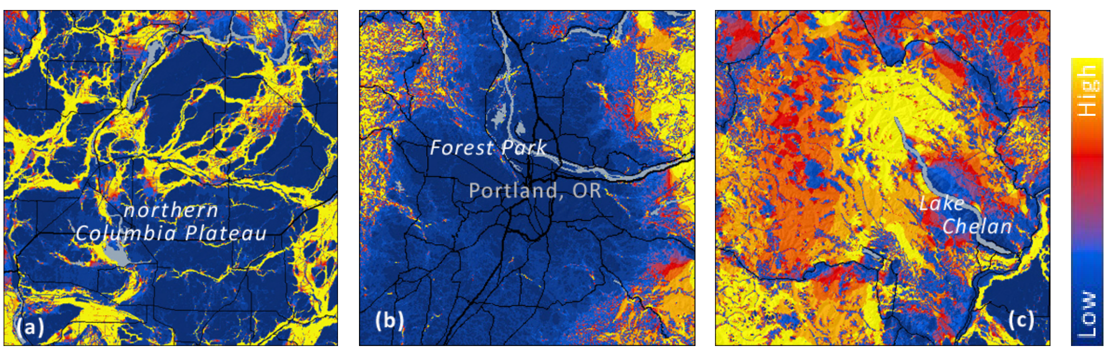

Figure 6. Current flow patterns in three landscapes with differing landscape composition. a) Current is channeled along natural features (flood-scoured channels in scablands) surrounded by agricultural lands in the Northern Columbia Plateau in eastern Washington. b) Current flow is all but blocked in the Portland, OR area, and there are relatively few natural areas to connect in the area, but some current concentrates in natural areas like Forest Park. c) Current flows around the northern end of Lake Chelan, WA, because open water and developed areas to the south have high resistance.

As with traditional Circuitscape results, diffuse flow in large, intact areas was harder to discern with these results. The moving window approach helped to highlight intact areas somewhat, because large natural areas have many sources and targets to connect. Still, local pinch-points tend to have even higher flow, overshadowing the more intact portions of our study area. Moreover, the flow through a given area is the product of two factors: the amount of natural land to connect within the search radius, and the configuration of movement routes available between those natural lands. The effects of these two factors can be difficult to distinguish within a single map of current flow, as low levels of flow can arise from several different mechanisms (e.g., spread of current across larger areas, fewer natural areas to connect, impeded flow, and proximity to coasts).

Because conservation strategies would potentially differ among these different contexts, it is important to try to distinguish their locations in the landscape. To help users do this, we produced two additional maps, representing *regional flow potential* and *normalized current flow*, respectively, designed to create more interpretable results. We describe these next.

Regional flow potential

To further distinguish intact (diffuse flow) areas from areas where flow is locally channeled, we developed a map of *regional flow potential*. By this we mean, *given the amount and configuration of natural pixels available to connect within 50 km, how much flow would be expected in the* absence *of barriers?* We produced this map by running the same OmniScape analysis but setting *all* resistances to the lowest score of 1. We used the same source weight raster to determine how much current flowed to and from pixels. As a result of these modifications, areas with higher current flow were located between larger expanses of natural land (i.e., areas that serve as sources or destinations for moving organisms), and thus flow indicates their potential to connect natural lands in the absence of barriers.

Map 5 shows results with all resistances set to the lowest score of 1. This map serves as a baseline, or *null model*, against which we can compare flow patterns impeded or channeled by landscape features. Pixels surrounded by highly natural areas, particularly those away from lakes and coasts, have the most natural land to connect within 50 km, and thus the highest flow potential. Areas where natural lands have been converted show lower flow potential, as do areas adjacent to large water bodies, because there are fewer natural lands to connect via those areas.

Normalized current flow

We divided current flow by regional flow potential to produce a map of *normalized current flow* (Map 6). This map helps to tease apart the mechanisms behind different flow rates, and better distinguishes broadly natural areas with diffuse flow from areas where barriers are blocking flow or channeling flow through pinch-points. If flow is lower than would be expected without barriers, then barriers are blocking flow from the area. This is evident in urban centers, which have low scores. If flow is higher than would be expected without barriers (i.e., current flow is high relative to regional flow potential), then barriers are channeling flow into the area and potentially creating pinch-points. These areas often show where the best movement options still exist in fragmented landscapes, e.g., in the scablands in the northern Columbia Plateau (Fig. 7a). In areas where barriers are having little effect on current flow patterns, current flow and regional flow potential will be approximately equal (i.e., the ratio of actual to expected flow will be close to 1). These are diffuse flow areas (Map 6).

Map 5: Regional Flow Potential

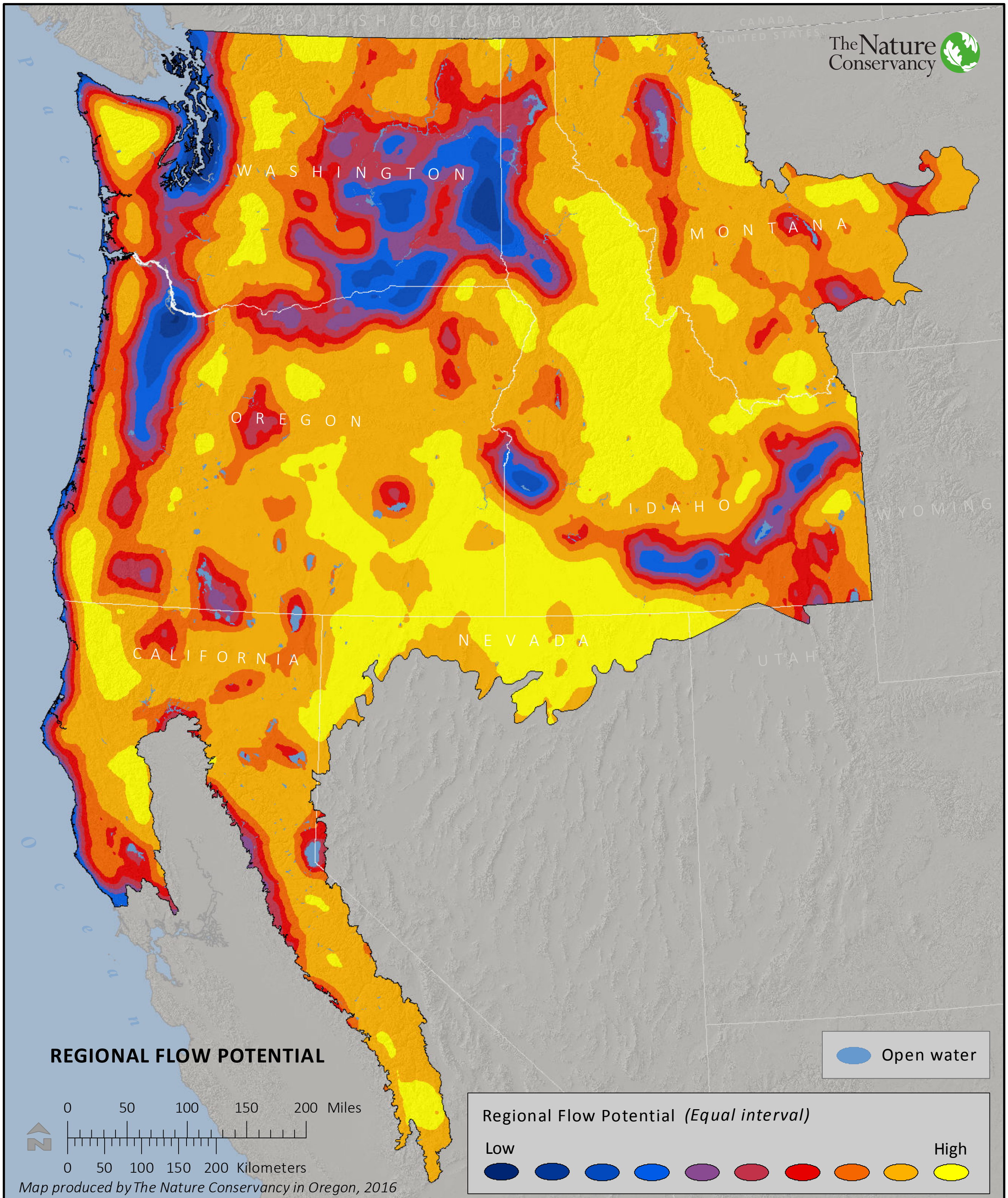

Given the amount and configuration of natural pixels available to connect within the analysis window, this map shows how much flow would be expected in the absence of barriers, which we term regional flow potential. The dataset was produced by running OmniScape with the original source-weight dataset and a null resistance surface with all cells assigned the lowest resistance of 1. Pixels surrounded by highly natural areas have the most natural land to connect within the search radius, and thus the highest flow potential.

Map 6: Regional Connectivity

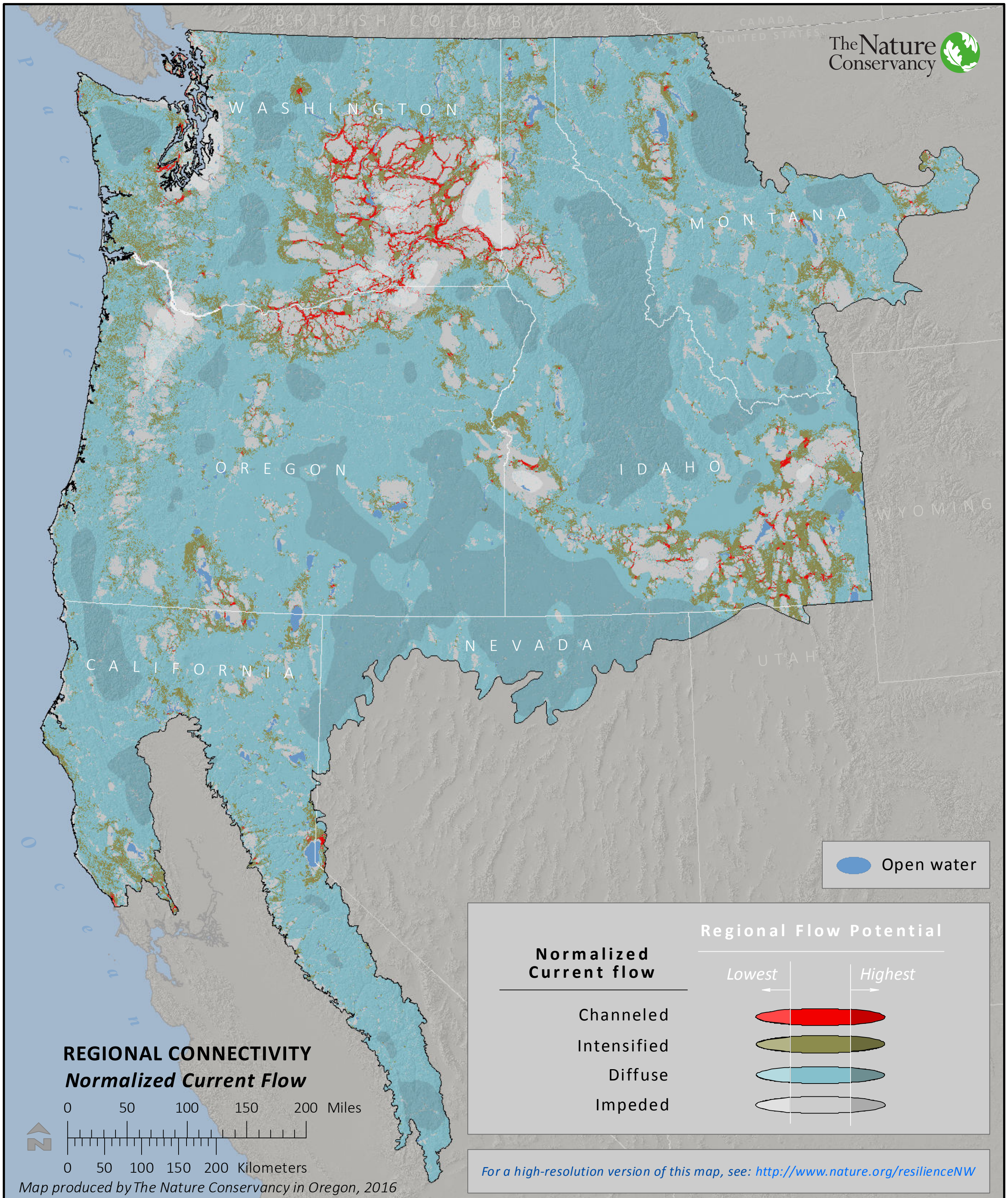

Integrating data from Maps 4 and 5 yields a fuller picture of regional connectivity patterns. Here, current flow (Map 4) was normalized by dividing it by regional flow potential (Map 5). Upper and lower extremes of regional flow potential are overlaid in order to highlight areas with the most and least natural land to connect, respectively. This helps to distinguish 1) broad, intact areas where movement is diffuse or largely unrestricted, 2) channeled areas or pinch points where further habitat loss could isolate natural areas, and 3) areas where flow is impeded by barriers.

Large, intact areas can be easily discerned using Maps 5 and 6. They have *high regional flow potential* in Map 5 and fall in the "diffuse" class in Map 6.

Pilot climate gradient analysis

Over longer timeframes, the degree to which landscapes are connected across climate gradients will likely be a key factor in mediating range shifts (Hannah et al. 2014, Nuñez et al. 2013). To demonstrate how our method can be adapted to explicitly incorporate climate, we conducted a pilot analysis that combined our algorithm with present-day climate data connecting each natural and semi-natural pixel to cooler pixels (if available) within 50 km (see Nuñez et al. 2013 for rationale behind climate gradient connectivity analyses). Similar to Nuñez et al. (2013), we used the 30-year mean of mean annual temperature (MAT); in our case, we used means from 1961 to 1990, available at 1 km^2 resolution from AdaptWest (AdaptWest Project 2015). In our study region, gradients in mean annual temperature are broadly correlated with those of more direct ecological relevance, such as growing-degree days, average temperature of the coldest month, and moisture deficit (Nuñez et al. 2013). We resampled our MAT layer to 180 m resolution, and connected pixels that differed by $\geq 1\ ^{\circ}C$ and $\leq 5\ ^{\circ}C$. We consider this an experimental application of our methods to demonstrate how they could be used with climate data; there are many data and parameter decisions that we did not have time to explore, such as use of climate data other than MAT, the use of more finely-downscaled climate data (as done by WHCWG 2013), and appropriate temperature differences to connect.

Map 7 shows current flow when only pixels that differ by 1-5 $^{\circ}C$ were connected. Compared with Map 4, flow is diminished in areas with fewer options for moving to significantly cooler areas within 50 km, e.g., portions of the Columbia Plateau and the Oregon Coast range.

Map 7: Current Flow across Climate Gradients

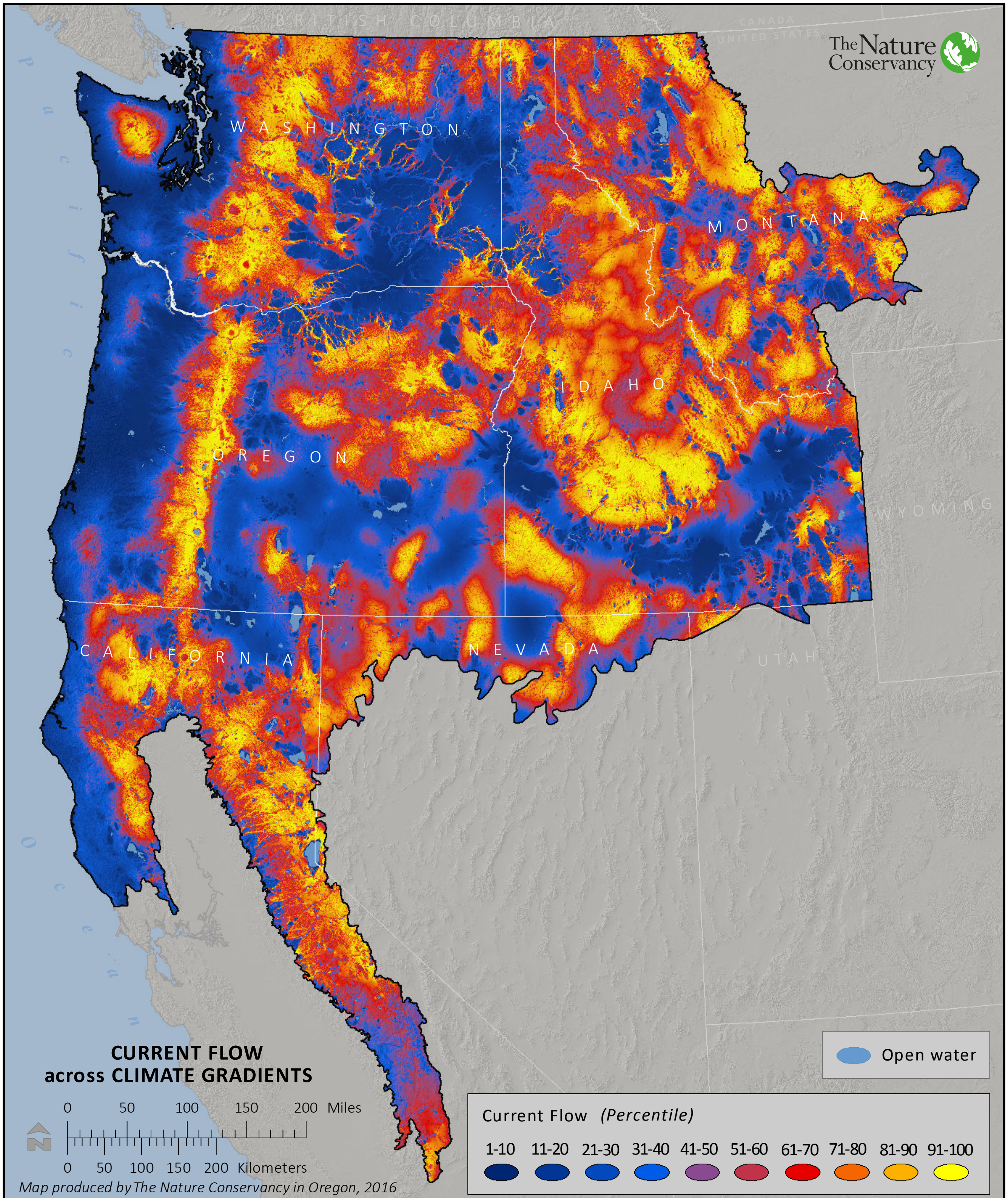

This map provides an early look at how incorporating climate data can change omnidirectional connectivity results. Current flow is used to predict movement routes from warm to cool areas across climate gradients. In this case, movement was allowed only between pixels where temperatures differed by 1-5 °C. We expect future OmniScape analyses will support investigation of areas likely to be important for connecting across climate gradients, between analogous present-day and projected future climates, and/or between present and projected future species ranges.

Discussion and Guidance for Use

As in previous applications of Circuitscape (e.g., Anderson et al. 2012, 2014, Koen et al. 2014, Pelletier et al. 2014), our maps can help to identify areas where landscape features are likely to block or constrain movement. Our methods allow us to explicitly define what is being connected, allowing more flow among more natural areas, while still preserving the ability to model connectivity in a continuous, core-free framework. This means that total current flow will be higher in natural landscapes than in more human-modified landscapes, and more flow will be modeled among large natural patches than among small ones.

Moreover, our ratio of flow to potential flow (Map 6) enhances the ability to highlight broadly connected lands where flow is likely to be unconstrained. These areas of diffuse flow through intact natural lands are typically difficult to distinguish in connectivity maps, but maintaining such areas may often be the most cost-effective way to maintain functioning natural landscapes.

Incorporating climate data: a pilot analysis

Although our results incorporating climate data (Map 7) can give users an idea of which portions of the study area could promote movement across significant climate gradients, we emphasize that this effort was experimental and more work needs to be done to determine the effects of data choices and decisions made parameterizing the model. For example, the temperature data we used are at a coarse spatial scale. Had we used climate data that included finer-scale topoclimatic variation, more temperature matches would have been found overall, including in areas with less-steep temperature gradients (Gillingham et al. 2012). Moreover, although gradients in mean annual temperature are correlated with biologically important gradients, different climatic variables are likely limiting for different species in different portions of our study area (Wang and Price 2007, Nuñez et al. 2013). Thus, this map should be considered a proof-of-concept rather than a definitive map of important areas for movement across climate gradients. Still, the map illustrates how explicitly modeling which areas would provide access to cooler climates might change prioritizations.

How to use these products

Maintaining well-connected landscapes is important for many processes, including daily movements, dispersal from natal areas, gene flow, recolonization of vacant habitat, and range shifts under climate change. These processes are highly complex and vary among species and types of movement. The areas important for conservation will depend on what is being connected, the process that is being conserved, and the timeframe over which that process is expected to occur.

Thus it is impossible to create a single map that captures all areas important for maintaining all types of connectivity. In this light, these products cannot be taken as simple maps of which areas are most important or which strategies are appropriate in different parts of the study area. Instead, we recommend that users carefully examine the maps and data layers provided, including current flow, regional flow potential, and normalized flow, as well as resistance and source weight maps. These maps can best guide conservation strategies when the user identifies what is being connected, understands how well the process to be conserved matches model assumptions, and combines the results with other priorities.

We suggest that these products may best be used to create narratives describing the connectivity value of different sites under consideration for conservation actions. For any area under consideration, our three connectivity maps (*current flow, potential flow, and normalized flow*) can be used in concert to help users consider not only the relative amount of ecological flow likely to be in the landscape, but what is being connected by that flow — natural lands, semi-natural lands, etc. Additional data can be combined with these products to determine whether high-flow areas cross climatic gradients, connect resilient lands, or connect habitat for particular species of concern.

In developing such narratives, we suggest users:

1) *Give special consideration to intact areas with high amounts of natural lands to connect.* These areas have high regional flow potential scores and normalized current flow levels that fall in the "diffuse" class across large areas. Examples include central Idaho, northern Nevada, southeastern Oregon, the Cascades in Washington, and the Kalmiopsis and Siskiyou areas of Oregon and California (Map 6).

2) *Carefully evaluate areas with channeled flow; these could indicate pinch-points.* High normalized flow scores indicate areas where flow has been channeled by barriers, and as such they often occur where landscapes are fragmented by water bodies or human development. Some of the clearest examples in our study area include the northern Columbia Plateau Ecoregion*,* where coulees and flood-scoured scablands form linear connections across large agricultural areas (Fig. 7a; see also WHCWG 2012); the Kitsap Peninsula, where a relatively small isthmus connects the peninsula to the mainland (Fig. 7b); and "halos" of high normalized flow where current skirts around agricultural areas, such as the Snake River Plain in Idaho (Fig. 7c).

   Pinch-points can indicate areas that are critical for maintaining connectivity — they may be the last routes connecting natural lands and their loss may sever such connections. But they must also be interpreted carefully. Because they are associated with fragmentation, flow through them may also be crossing barriers or traveling large distances to circumvent barriers. Recall that in our model, current may pierce a barrier if it represents the best route possible.

   Users should carefully evaluate the viability of connections through pinch-points, and consider whether they are viable targets for protection (to maintain their existing connectivity functions) or restoration (to provide alternate routes and alleviate constrictions in flow). Restoration should also be considered where high flow crosses restorable barriers.

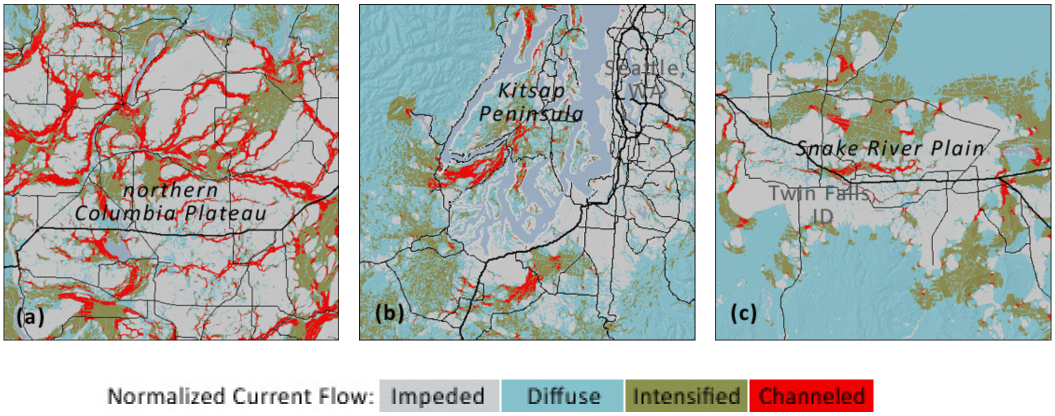

Figure 7. Examples of high normalized flow scores, where flow has been channeled by natural or anthropogenic barriers. a) The northern Columbia Plateau Ecoregion*,* where coulees and flood-scoured scablands form linear connections across large agricultural areas. b) The Kitsap Peninsula, where a relatively small isthmus connects the peninsula to the mainland. c) 'Halos' of high normalized flow where current skirts around the Snake River Plain in Idaho.

3) *Pay attention to intact coastal areas*. Coastal areas typically show low amounts of flow (e.g., Fig. 5c) and also score low on regional flow potential, because by definition they don't fall between large concentrations of natural lands. Centrality approaches such as ours will discriminate against such areas, but for many reasons connecting coasts to inland areas may still be an important conservation goal. The normalized flow map helps identify coastal areas with high degrees of naturalness and normalized flow scores in the "diffuse" class, indicating opportunities for achieving this.

4) *Compare results with local permeability analyses*. Many of the same patterns in our results can also be detected in the local permeability results (Map 7.2 in Buttrick et al. 2015); in particular, both will allow users to detect large, intact areas and highly converted areas. But this broad-scale connectivity analysis emphasizes how areas contribute to connectivity over larger distances, thus providing complementary information. Areas of agreement between the two approaches should be given extra consideration.

5) *Compare results with terrestrial resilience data to identify resilient linkages and/or linkages between resilient areas.* Similar to other examples, areas where the two analyses agree (i.e., a resilient area that also has good connectivity) should be given special consideration (Map 8). Linkages between high-resilience areas may also be very important, especially if alternative movement routes do not exist. One example of this is in the Columbia Plateau region of eastern Washington (Fig. 8), where flood-scoured scablands connect resilient areas, with these linkages identified in the regional connectivity data as intensified or channeled. These linkages also connect areas differing in mean annual temperature (Map 7), and protection or restoration could provide multiple conservation benefits.

Map 8: Regional Connectivity and Terrestrial Resilience Density

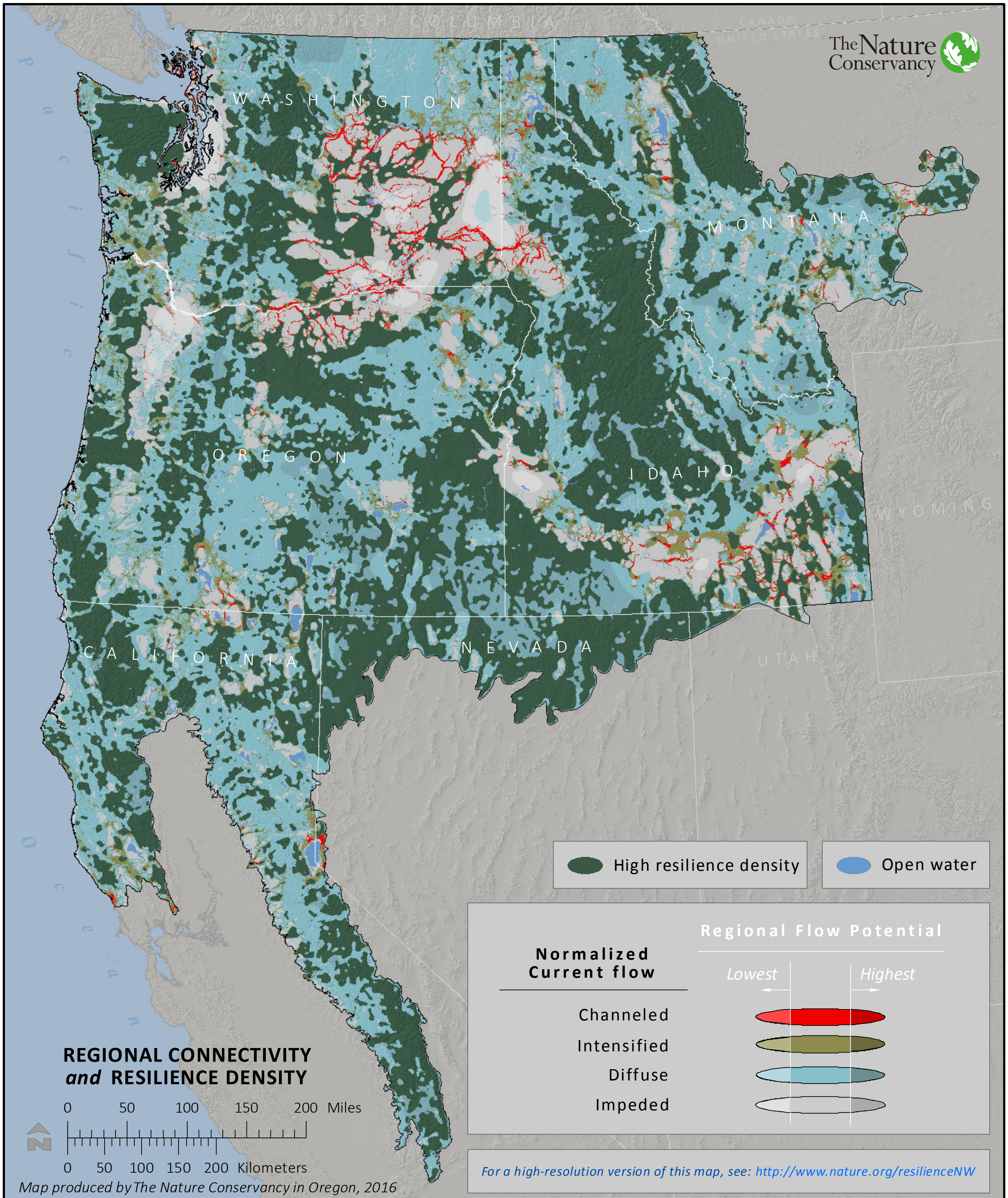

This map overlays results of this analysis with resilience data from Buttrick et al. (2015). Areas with above-average terrestrial resilience are shown on top of the regional connectivity results from Map 6. This provides one example of how connectivity data can be combined with other priorities, in this case showing linkages that may be important for connecting highly resilient areas.

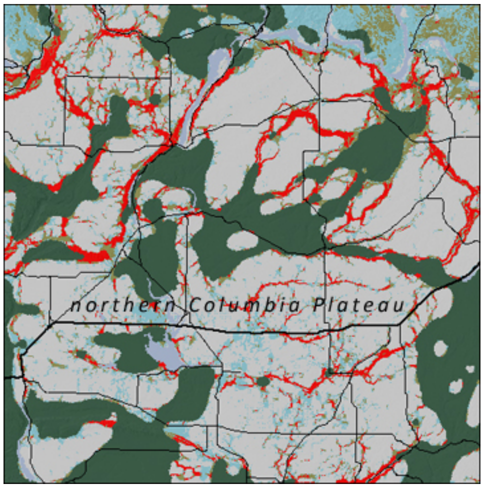

Figure 8. Areas with above-average resilience overlaid on connectivity results in the northern Columbia Plateau. Combining our results with previous analyses or other prioritizations can help inform conservation decisions. In this case, linkages that connect highly resilient sites are identified.

6) *Consider other sources of connectivity information*. Independent analyses of connectivity (e.g., WHCWG 2010, 2013, Krosby et al. 2014, Littlefield et al. in review), movement data, or landscape genetic data can complement these analyses, particularly to support species-specific conservation efforts. Users should place more confidence in areas where different modeling efforts agree, and more weight should be given to conservation actions supported by different analytical approaches, data sources, or conservation goals (e.g., restoration of riparian habitat in an area identified by multiple analyses as important for connectivity or climate resilience).

7) *Consider other priorities.* Similar to the rest of the Conserving Nature's Stage methodology and datasets (www.nature.org/resilienceNW), it is possible to use these data in concert with almost any other prioritization dataset. Identifying which portions of existing protected areas are most at risk of losing connectivity, which unprotected areas may be most important to connect, where the most connected areas are for a potential species reintroduction programs, or which areas are most important to prioritize for improved management because they demonstrate high connectivity value are but a few of the myriad of ways these data could be combined with other conservation priorities.

Caveats and potential enhancements

As with many connectivity analyses (e.g., WHCWG 2010, 2012), modeled routes may pass over barriers and these routes must be evaluated for viability. As described earlier in this report, current in our model will take the best route possible to connect all sources and targets within 50 km of one another, and will "bore through" barriers if alternative, low-resistance routes are unavailable. Similarly, current will flow distances greater than 50 km – as long as they remain within the circular window – to reach targets. Thus, careful interpretation and on-the-ground validation of movement routes should be conducted before conservation actions are taken.

Both the resistance and source-weight modeling processes relied on expert opinion, involving many subjective decisions, and we emphasize that no single resistance or naturalness scoring scheme will be ideal for all individual species of conservation concern. Rather, our model focuses on keeping natural lands structurally connected to one another via the most natural movement routes, focusing on connecting the "stages" upon which a diverse set of species are most likely to be found now and into the future (Buttrick et al. 2015). Users should carefully examine our resistance and naturalness score maps to determine the degree to which the maps are compatible with their conservation goals. We further note that we considered large water bodies to be significant barriers, did not consider effects of steep terrain (including cliffs), and connected pixels among dramatically different vegetation types and biomes. These are all modeling decisions that could have been made differently depending on goals and assumptions.

An example of how our models are sensitive to resistance scores and other parameters is the previously mentioned zone of high flow to the north of Lake Chelan (Fig. 6c). This zone exists because we are connecting large blocks of natural land on opposite sides of the lake. Moving windows completely encircle the lake, and current tends to flow around the northern tip of the lake from sources on one side to the other because open water has high resistance and movement around the southern end of the lake is hindered by roads and the town of Chelan and roads. Moreover, flow farther north is somewhat impeded by Ross Lake and US Highway 20 (Fig. 6c). Thus, flow between eastern and western sides of the lake is somewhat constrained and concentrated at the northern tip. This pattern would be diminished had we limited the total linear distance that current could travel, or had we used a lower resistance for open water (because more current would have flowed across the lake rather than around it).

Note that "channeled"/"intensified"/"diffuse"/"impeded" designations based on our normalized current scores are scaled based on how much natural land is available to connect, and this varies considerably across our study area. As such, the results shown in Map 6 must be viewed in context and in conjunction with those shown in Maps 4 and 5. For example, roads within channeled areas may have normalized current scores close to 1 (placing them in the "diffuse" class), simply because flow is locally avoiding them and thus their flow scores are more in line with expectations based on regional potential.

Our moving window method is experimental, but is promising in several respects. First, it readily identifies where large concentrations of intact natural lands exist, and where organisms occupying natural lands could move a user-specified distance to reach other natural areas. Second, it produces continuous maps and does not require identifying discrete patches of natural lands to connect. Third, the moving window method is flexible, with potential for many additional enhancements.

- Current flow could be scaled such that flow is lower from sources that are more distant from targets. For example, within a 50-km window, sources 5 km from the target would produce more flow to the target than sources 40 km from the target.

- For species-specific applications, source weights could reflect habitat suitability rather than naturalness, resulting in more flow modeled between large, high-quality habitat blocks than between smaller or lower-quality blocks.
- In specific climate connectivity applications, the method could be used to connect across climate gradients (as in our example in Map 7 and in an early application of our code by Anderson et al. 2015), or present-day climate data and future climate projections could be used to connect pixels to targets that have analogous climates under future projections (as in Littlefield et al. in review).
- Connectivity along riparian and freshwater habitats could be modeled by limiting analyses to only those habitat types. Alternatively, flow through riparian areas and valley bottoms could be extracted from our results and examined separately to identify riparian areas that contribute highly to regional connectivity.
- Flow from sources could be scaled with cost distance or effective resistance, so that current would be diminished between sources and targets separated by strong barriers. In the present analysis, total current leaving a source was not affected by movement difficulty, but simply flowed along the best route possible, even if that route crossed strong barriers.
- Restoration opportunities could be evaluated in two ways. Voltage maps (see McRae et al. 2008) could be produced by the algorithm and used to identify restoration opportunities as suggested in McRae et al. (2012); such applications require further exploration. More simply, the model could be rerun with a set of proposed restoration projects burned into the resistance layer to evaluate how connectivity values could change following restoration.

Data Products

Data, maps, and computer code created by this project are included in a small set of files available for download from this Conservation Gateway site http://nature.org/resilienceNW along with any updates to this report.

Report, Appendices and Maps

Two files are available which include:

1. The main report and written appendices.
2. High-resolution (600 dpi) versions of the report maps.

GIS data

GIS data created for the project, including resistance, source weight, and currentflow maps, are available at www.nature.org/resilienceNW.

Scripts

Computer code created for the project, including OmniScape and land cover pre-processing scripts, are available upon request. Please see www.nature.org/resilienceNW for contact information.

Literature Cited

AdaptWest Project. 2015. Gridded current and projected climate data for North America at 1-km resolution, interpolated using the ClimateNA v5.10. Available at adaptwest.databasin.org.

Anderson, M. G., A. Barnett, M. Clark, C. Ferree, A. Olivero Sheldon, and J. Prince. 2014a. Resilient Sites for Terrestrial Conservation in the Southeast Region. The Nature Conservancy, Boston, MA.

Anderson, M. G., M. Clark, and B. H. McRae. 2015a. Permeable Landscapes for Climate Change. The Nature Conservancy, Boston, MA.

Anderson, M. G., M. Clark, and A. O. Sheldon. 2012. Resilient Sites for Terrestrial Conservation in the Northeast and Mid-Atlantic Region. The Nature Conservancy, Eastern Conservation Science. The Nature Conservancy, Boston, MA.

Anderson, M. G., M. Clark, and A. O. Sheldon. 2014b. Estimating climate resilience for conservation across geophysical settings. Conservation Biology 28:959–970.

Anderson, M. G., P. J. Comer, P. Beier, J. J. Lawler, C. A. Schloss, S. Buttrick, C. M. Albano, and D. P. Faith. 2015b. Case studies of conservation plans that incorporate geodiversity. Conservation Biology 29:680–691.

Beier, P., M. Hunter, and M. Anderson. 2015. Special section: Conserving nature's stage. Conservation Biology 29:613–617.

Blois, J. L., P. L. Zarnetske, M. C. Fitzpatrick, and S. Finnegan. 2013. Climate change and the past, present, and future of biotic interactions. Science 341:499–504.

Brodie, J. F., A. J. Giordano, B. Dickson, M. Hebblewhite, H. Bernard, J. Mohd-Azlan, J. Anderson, and L. Ambu. 2015. Evaluating multispecies landscape connectivity in a threatened tropical mammal community. Conservation Biology 29:122–132.

Buttrick, S., K. Popper, M. Schindel, B. H. McRae, B. Unnasch, A. Jones, and J. Platt. 2015. Conserving Nature's Stage: Identifying Resilient Terrestrial Landscapes in the Pacific Northwest. The Nature Conservancy, Portland, Oregon.

Chen, I.-C., J. K. Hill, R. Ohlemüller, D. B. Roy, and C. D. Thomas. 2011. Rapid range shifts of species associated with high levels of climate warming. Science 333:1024–1026.

Commission for Environmental Cooperation (CEC). 2013. 2010 North American Land Cover at 250 m spatial resolution. Produced by Natural Resources Canada/Canadian Center for Remote Sensing (NRCan/CCRS), United States Geological Survey (USGS); Insituto Nacional de Estadística y Geografía (INEGI), Comisión Nacional para el Conocimiento y Uso de la Biodiversidad (CONABIO) and Comisión Nacional Forestal (CONAFOR).

Compton, B. W., K. McGarigal, S. A. Cushman, and L. R. Gamble. 2007. A Resistant-Kernel Model of Connectivity for Amphibians that Breed in Vernal Pools. Conservation Biology, 21:788-799.

Corlett, R. T., and D. A. Westcott. 2013. Will plant movements keep up with climate change? Trends in Ecology and Evolution 28:482–488.

Crimmins, S. M., S. Z. Dobrowski, J. A. Greenberg, J. T. Abatzoglou, and A. R. Mynsberge. 2011. Changes in climatic water balance drive downhill shifts in plant species' optimum elevations. Science 331:324–327.

Dickson, B. G., G. W. Roemer, B. H. McRae, and J. M. Rundall. 2013. Models of regional habitat quality and connectivity for pumas (Puma concolor) in the Southwestern United States. PLoS ONE 8.

Dutta, T., S. Sharma, B. H. McRae, P. Roy, and R. DeFries. 2015. Connecting the dots: mapping habitat connectivity for tigers in central India. Regional Environmental Conservation:1–15.

Gill, J. L., J. L. Blois, B. Benito, S. Dobrowski, M. L. Hunter, and J. L. Mcguire. 2015. A 2.5-million-year perspective on coarse-filter strategies for conserving nature's stage. Conservation Biology 29:640–648.

Gillingham, P. K., Palmer, S. C., Huntley, B., Kunin, W. E., Chipperfield, J. D. and Thomas, C. D. 2012. The relative importance of climate and habitat in determining the distributions of species at different spatial scales: a case study with ground beetles in Great Britain. Ecography 35:831-838.

Hannah, L., L. Flint, A. D. Syphard, M. A. Moritz, L. B. Buckley, and I. M. McCullough. 2014. Fine-grain modeling of species' response to climate change: Holdouts, stepping-stones, and microrefugia. Trends in Ecology and Evolutionrends in Ecology and Evolution 29:390–397.

Heller, N. E., and E. S. Zavaleta. 2009. Biodiversity management in the face of climate change: A review of 22 years of recommendations. Biological Conservation 142:14–32.

Hoffmann, A., and C. Sgrò. 2011. Climate change and evolutionary adaptation. Nature 470:479–485.

Jackson, S. T., and J. T. Overpeck. 2000. Responses of plant populations and communities to environmental changes of the late Quaternary. Paleobiology 26:194–220.

Jin, S., Yang, L., Danielson, P., Homer, C., Fry, J., and Xian, G. 2013. A comprehensive change detection method for updating the National Land Cover Database to circa 2011. Remote Sensing of Environment, 132: 159-175.

Krosby, M. B., R. Norheim, D. M. Theobald, and B. McRae. 2014. Riparian Climate-Corridors: Identifying Priority Areas for Conservation in a Changing Climate. Climate Impacts Group, University of Washington, Seattle, WA.

Krosby, M., J. Tewksbury, N. M. Haddad, and J. Hoekstra. 2010. Ecological connectivity for a changing climate.

Lawler, J. J., D. D. Ackerly, C. M. Albano, M. G. Anderson, S. Z. Dobrowski, J. L. Gill, N. E. Heller, R. L. Pressey, E. W. Sanderson, and S. B. Weiss. 2015. The theory behind, and the challenges of, conserving nature's stage in a time of rapid change. Conservation Biology 29:618–629.

Lawler, J. J., A. S. Ruesch, J. D. Olden, and B. H. McRae. 2013. Projected climate-driven faunal movement routes. Ecology Letters 16:1014–1022.

Littlefield, C. E., B.H. McRae, J. Michalak, J. J. Lawler, and C. Carroll. (In review). Missed connections: Tracking climates through time and space to predict connectivity under climate change. Conservation Biology.

Loarie, S. R., P. B. Duffy, H. Hamilton, G. P. Asner, C. B. Field, and D. D. Ackerly. 2009. The velocity of climate change. Nature 462:1052–1055.

McGuire, J. L., J. J. Lawler, B. H. McRae, T. Nuñez, and D. M. Theobald. 2016. Achieving climate connectivity in a fragmented landscape. Proceedings of the National Academy of Sciences of the United States of America.

McRae, B. H., B. G. Dickson, T. H. Keitt, and V. B. Shah. 2008. Using circuit theory to model connectivity in ecology, evolution, and conservation. Ecology 89:2712–2724.

McRae, B. H., S. A. Hall, P. Beier, and D. M. Theobald. 2012. Where to restore ecological connectivity? Detecting barriers and quantifying restoration benefits. PLoS ONE 7.

McRae, B. H., V. B. Shah, and T. K. Mohapatra. 2013a. Circuitscape 4 User Guide. The Nature Conservancy, Fort Collins, CO.

McRae, B.H., A.J. Shirk, and J.T. Platt. 2013b. Gnarly Landscape Utilities: Resistance and Habitat Calculator User Guide. The Nature Conservancy, Fort Collins, CO. Available at: http://www.circuitscape.org/gnarly-landscape-utilities.

Meiklejohn, K., R. Ament, and G. Tabor. 2009. Habitat Corridors & Landscape Connectivity: Clarifying the Terminology. Center for Large Landscape Conservation, Bozeman, MT.

Moritz, C., and R. Agudo. 2013. The future of species under climate change: resilience or decline? Science 341:504–508.

Noss, R. F. 1987. From plant communities to landscapes in conservation inventories: A look at the nature conservancy (USA). Biological Conservation 41:11–37.

Nuñez, T. A., J. J. Lawler, B. H. McRae, D. J. Pierce, M. B. Krosby, D. M. Kavanagh, P. H. Singleton, and J. J. Tewksbury. 2013. Connectivity planning to address climate change. Conservation Biology 27:407–416.

Rapacciuolo, G., S. P. Maher, A. C. Schneider, T. T. Hammond, M. D. Jabis, R. E. Walsh, K. J. Iknayan, G. K. Walden, M. F. Oldfather, D. D. Ackerly, and S. R. Beissinger. 2014. Beyond a warming fingerprint: Individualistic biogeographic responses to heterogeneous climate change in California. Global Change Biology 20:2841–2855.

Schloss, C. a., T. a. Nunez, and J. J. Lawler. 2012. Dispersal will limit ability of mammals to track climate change in the Western Hemisphere. Proceedings of the National Academy of Sciences 2012:1–6.

Sexton, J. P., S. Y. Strauss, and K. J. Rice. 2011. Gene flow increases fitness at the warm edge of a species' range. Proceedings of the National Academy of Sciences 108:11704–11709.

Sgrò, C. M., A. J. Lowe, and A. A. Hoffmann. 2011. Building evolutionary resilience for conserving biodiversity under climate change. Evolutionary Applications 4:326–337.

Thomas, C. D. 2010. Climate, climate change and range boundaries. Diversity and Distributions 16:488–495.

Thuiller, W., S. Lavorel, M. B. Araujo, M. T. Sykes, and I. C. Prentice. 2005. Climate change threats to plant diversity in Europe. Proceedings of the National Academy of Sciences 102:8245–8250.

Vasudev, D., and R. J. Fletcher. 2015. Incorporating movement behavior into conservation prioritization in fragmented landscapes: An example of western hoolock gibbons in Garo Hills, India. Biological Conservation 181:124–132.

Wang, A., and D. T. Price. 2007. Estimating global distribution of boreal, temperate, and tropical tree plant functional types using clustering techniques. Journal of Geophysical Research-Biogeosciences 112.

Warren, M. S., J. K. Hill, J. A. Thomas, J. Asher, R. Fox, B. Huntley, D. B. Roy, M. G. Telfer, S. Jeffcoate, P. Harding, G. Jeffcoate, S. G. Willis, J. N. N. Greatorex-Davies, D. Moss, and C. D. Thomas. 2001. Rapid responses of British butterflies to opposing forces of climate and habitat change. Nature 414:65–69.

Washington Wildlife Habitat Connectivity Working Group (WHCWG). 2010. Washington Connected Landscapes Project: Statewide Analysis. Washington Departments of Fish and Wildlife and Transportation, Olympia, WA.

Washington Wildlife Habitat Connectivity Working Group (WHCWG). 2012. Washington Connected Landscapes Project: Analysis of the Columbia Plateau Ecoregion. Washington Departments of Fish and Wildlife and Department of Transportation, Olympia, WA.

Washington Wildlife Habitat Connectivity Working Group (WHCWG). 2013. Washington Connected Landscapes Project: Columbia Plateau Climate-Gradient Corridors Analysis. Washington Departments of Fish and Wildlife and Department of Transportation, Olympia, WA.

Appendix A: Description of Resistance and Source Weight Modeling

Several datasets and processing steps were used in the creation of the resistance and source weight layers. Although most of these datasets had been used in our earlier local permeability analysis (Buttrick et al. 2015), the search larger radius required to model regional connectivity (50 km vs 3 km) necessitated refreshing all datasets to increase their extent into a buffer region around our study area to prevent edge effects.

The same general processing workflow was also followed, with some enhancements, from the 2015 local permeability analysis. A wall-to-wall land-cover map was created as the basis of the resistance and source weight surfaces. These base land-cover layer were then augmented with finer-scaled data, such as data on electrical transmission lines and roads, from ancillary datasets. This approach allowed us to incorporate the best local data for many of the important features that can affect terrestrial regional connectivity.

Base land-cover data

To mitigate for edge effects, the base land-cover data needed to extend well beyond our project footprint. Within the U.S., the 2011 National Land Cover Dataset (NLCD; Jin et. al. 2013) covered the entire project area including the buffer. However, the buffer region north of the international boundary was not represented. To fill this gap, we used the Canadian portion of the North American Land Cover Dataset (Commission for Environmental Cooperation 2013). These data were resampled from their native 250-m pixel size to match the 30-m pixel size of the NLCD, then reclassified to crosswalk to the land-cover class values in NLCD. These two datasets were then merged as the basis for subsequent processing.

To maximize the benefits of incorporating ancillary data it was first necessary to remove the vestiges of those that appeared in the land-cover map, especially roads. NLCD, for example, inconsistently represented roads as various developed types, and missed many altogether. These road artifacts were problematic for two reasons. First, existing road fragments were assigned to various development classes, with differing resistance scores, which would erroneously affect resistance values. Second, any misalignment between datasets would allow double-counting of roads in cases where multiple parallel road features appeared in the final data layer.

Similarly, bridges over water bodies often appear in land-cover data, complicating our efforts to develop a resistance model that included information on distance from shore. Without removing bridges from land-cover data, water pixels adjacent to bridges could not be distinguished from water pixels adjacent to shore.

To remedy these issues, as well as to reclassify water into distance bands to represent increasing difficulty many terrestrial species would experience when crossing wider bodies of water, we developed a python script. The first task the script performed was to reclassify water bodies in the NLCD/NALC layer to include information on distance from shore. This necessitated first removing bridges, so that water pixels adjacent to bridges would not be assigned to low distance classes. We used a modification of methods used to remove roads by the Washington Wildlife Habitat Connectivity Working Group (WHCWG 2013). This was accomplished with the ArcGIS *Shrink* command, which we used to contract all developed areas by 2 pixels, replacing those cells with their nearest neighbor values. This resulted in a land-cover map with bridges removed. The script then removed "barren" and "herbaceous wetland" classes (which in many cases corresponded to tidal flats or sand bars), and calculated Euclidean distances from the nearest remaining non-water classes. Water pixels in the original NLCD/NALC layer were then reclassified to reflect these Euclidean distances, creating a new water raster with classes representing several distance bands. Note that this meant that water pixels immediately adjacent to urban pixels were assigned to higher distance classes because urban areas were shrunk by two pixels. This allowed us to later penalize movements through pixels immediately adjacent to urban shorelines, which would have provided unrealistically conducive movement routes skirting developed shorelines.

The second task the script performed was to remove roads from the original NLCD/NALC layer, using both the ArcGIS *Shrink* and *Expand* commands. As with removing bridges, we removed roads using the *Shrink* operation, but in this case only contracting by one pixel and then re-expanding remaining developed pixels back into their pre-contracted locations up to a distance of one pixel. In other words, if there were developed pixels that were shrunk but immediately adjacent to developed pixels that remained after the *Shrink* operation, the pre-shrunken pixels were re-assigned their original developed class. This process eliminated developed features less than two pixels wide but retained them otherwise. Thus, we were able to remove roads without losing developed pixels at the edges of urban or other developed areas. Shrunken developed pixels were assigned new codes identifying their original and replacement cover types (e.g., 21041 for pixels originally in class 21, "Developed, open space," that had been contracted and replaced by class 41, "Deciduous forest"). These unique codes allowed us to assign appropriate resistance values to each combination of pre- and post-process land-cover types.

Other data sources

To represent features that were not captured in our base land-cover data, we incorporated several additional datasets. These data represented features that were not well represented in the NLCD/NALC dataset, such as roads, energy infrastructure, and low-density housing. Each of these vector datasets was converted to a 30m raster and snapped to the base land-cover grid.

Roads were represented by multiple datasets. TIGER roads data (U.S. Census Bureau 2013) were available for the entire USA, and these were used to identify freeways and highways, as well as low-use roads. However, we found that low-use roads were incomplete in this dataset. This is problematic because in rural, non-agricultural areas away from highways and buildings, low-use roads are often the only readily mapped features that indicate human land uses. We therefore included roads data from the USDA Forest Service, the Bureau of Land Management, the California Timber Harvest Program, the State of Idaho, and the Canadian National Road network. In each case, we dropped the relatively small portion of road segments that were clearly identified as closed or decommissioned. No one dataset was comprehensive for any state, so we used all datasets that were of reasonable quality in combination.

Railroads were captured from the U.S. Census Bureau's 2013 TIGER database. Railroads include main, spur, and yard rail lines; carline, streetcar track, monorail, and mass transit lines; and cog rail line, incline rail, and tram lines. No rail lines were represented in the Canadian buffer zone.

Energy infrastructure, including all significant transmission lines, wind towers and natural gas pipelines within the U.S. portion of the project extent, were represented by the EV Energy Map layer (Ventyx 2015). Transmission lines in these data are grouped into voltage classes, so each could be given unique resistance weights reflecting the differing footprints on the landscape from different transmission capacities. Energy infrastructure was not represented in the Canadian portions of the buffer zone.

The 2010 *Population and Housing Unit Counts* Report, produced by the U.S. Census Bureau, were used in conjunction with census tract polygons (clipped to private lands) to calculate 8 classes of "Block Housing Density" (BHD) on private lands across the study area. These data, obtained from David Theobald (Conservation Science Partners), were included to represent the non-specific impacts associated with increasing human densities. As described in our 2015 report, housing densities are a good surrogate for a number of anthropogenic impacts, such as noise, predation by pets and non-native landscaping that reduce connectivity potential and which don't appear in standard land-cover classifications.

Resistance scores

We developed expert-based resistance scores for all classes in each input layer, representing the estimated resistance to movement created by each landscape feature (Appendix B). Resistance values for the 2015 local permeability analyses were based on accumulated cost-weighted distances (Compton et al. 2007). However, circuit-theoretic analyses are based on probabilities of a random walker moving into a pixel, so resistance values developed for one framework are not necessarily appropriate for the other. More work needs to be done to determine best practices for assigning resistance scores to different features; however, based on previous experience with broad-scale connectivity analyses (e.g., WHCWG 2010, 2013) and previous experience with developing resistance scores for Circuitscape, we developed a steeper scoring scheme to create more differentiation between permeable and impermeable land cover types. We began with scores that were roughly the square of values used in the previous permeability analyses, adjusting scores as needed to achieve values deemed appropriate for a circuit-theoretic framework. In the end, entirely "natural" pixels were assigned a resistance of 1, and anthropogenic or natural barriers were assigned resistances up to a maximum of 1000.

In most cases, highly resistant features were either only represented in a single dataset, or overlapped in ways that one dataset would "eclipse" the other (e.g., urban classes from NLCD and housing density classes from BHD). However, our road data were compiled from many sources with varying degrees of overlap. Because our resistance values are derived by taking the maximum, rather than the sum, of resistances from overlapping layers, having the same road represented in more than one layer would yield the same resistance values as long as the pixels aligned. However, misalignment between these source data often caused the same road to be represented in slightly different positions in the various datasets, typically running parallel within 30m, but sometimes farther apart.

To mitigate the effects of these misalignments, we maintained the target resistance of 9 for low-use roads, but spread the resistance across a larger area (90 m instead of 30 m). We accomplished this by reducing low-use roads resistance from 9 to 3, but assigned the value of 3 to roads that had been expanded (widened) by one 30-m pixel in each direction (resulting in a total resistance of 9 for crossing a road). This expansion meant that a single road represented as two side-by-side features from different road data layers typically had a large proportion of overlapping pixels from the two datasets. The extra resistance from parallel features was thus reduced except for a minority of cases where misalignment was greater than 60 m.

We were not concerned about these issues for roads in cities and towns, as urban features in the housing density and NLCD layers represent higher resistance values than low-use roads, and thus took precedence in those areas. Major roads and highways were still derived from a single dataset (TIGER), and assigned high resistances. Shrunken developed features in the NLCD/NALC were assumed to be low-use roads and were typically assigned either the resistance of low-use roads or the class that replaced the shrunken pixels, whichever was higher.

All scores were recorded in a Microsoft Excel spreadsheet, which referenced the layer, class, and resistance score. These data were input into the Resistance and Habitat Calculator of Gnarly Landscape Utilities (McRae et al. 2013b, http://www.circuitscape.org/gnarly-landscape-utilities). Road features were 'fattened' using the 'expand cells' setting (see details on low-use road treatment above). The resulting raster represented the maximum resistance across all input layers at a 30 m pixel size. We then aggregated to 180 m taking the mean value of all 30-m pixels within each 180-m pixel to produce our final resistance surface.

Source weights

As described in the main report, our approach required that each pixel be given a source weight, representing the weight that would be given to connections to and from that pixel (i.e., the amount of flow to and from the pixel). We gave greater source weights to land uses we considered to be more likely to support natural populations now or in the future, resulting in more current flowing to and from them. Pixels consisting of entirely natural vegetation were given the highest weight of 1, and entirely developed pixels were given a weight of zero. Semi-natural pixels that had some likelihood of supporting native species now or in the future were given intermediate values; for example, the NLCD "pasture/hay" class was given a source weight of 0.5, and croplands were given a value of 0.2. Unvegetated but still natural pixels were treated somewhat differently. "Perennial snow/ice" was given a value of 0.75, reflecting the assumption that these areas are inhospitable to most species now, but may become snow and ice free under climate change and thus become targets for range shifts. “Barren lands” in NLCD were also given a value of 0.75, since these often represent tidal areas or sand bars and in some cases are barren due to human land uses such as mining. “Open water” pixels were not considered sources or targets for movement, and were assigned a source weight of 0.

As with resistance modeling, shrunken developed features in NLCD/NALC data were assumed to be low-use roads. These were typically assigned either the source weight of low-use roads or the class that replaced the shrunken pixels, whichever was lower.

These data were input into a modified version of the Resistance and Habitat Calculator of Gnarly Landscape Utilities, producing a source raster reflecting the minimum source weight across all input layers at a 30m pixel size. The modification allowed us to fatten road features while taking the minimum value across inputs. We then aggregated to 180 m taking the mean value of all 30-m pixels within each 180-m pixel to produce our final source weight surface.

Appendix B: Resistance and Source Weight scores

Table B1. Source weight and resistance scores assigned to different classes in input layers.

Data Layer	Class ID	Class Description	Source wt	Resistance	Expand Cells
NLCD2011_NALC2010	11	Water	0	4	0
NLCD2011_NALC2010	12	Perennial Ice/Snow	0.75	2	0
NLCD2011_NALC2010	21	Developed, Open Space	0.3	16	0
NLCD2011_NALC2010	22	Developed, Low Intensity	0.2	81	0
NLCD2011_NALC2010	23	Developed, Medium Intensity	0.1	400	0
NLCD2011_NALC2010	24	Developed, High Intensity	0	1000	0
NLCD2011_NALC2010	31	Barren Land	0.75	2	0
NLCD2011_NALC2010	41	Deciduous Forest	1	1	0
NLCD2011_NALC2010	42	Evergreen Forest	1	1	0
NLCD2011_NALC2010	43	Mixed Forest	1	1	0
NLCD2011_NALC2010	52	Shrub/Scrub	1	1	0
NLCD2011_NALC2010	71	Grassland/Herbaceous	1	1	0
NLCD2011_NALC2010	81	Pasture/Hay	0.5	16	0
NLCD2011_NALC2010	82	Cultivated Crops	0.2	49	0
NLCD2011_NALC2010	90	Woody Wetlands	1	1	0
NLCD2011_NALC2010	95	Emergent Herbaceous Wetlands	1	1	0
NLCD2011_NALC2010	21011	Shrunken from 21 to Open Water	0	4	0
NLCD2011_NALC2010	21012	Shrunken from 21 to Perennial Ice/Snow	0.75	3	0
NLCD2011_NALC2010	21031	Shrunken from 21 to Barren Land	0.75	3	0
NLCD2011_NALC2010	21041	Shrunken from 21 to Deciduous Forest	0.75	3	0
NLCD2011_NALC2010	21042	Shrunken from 21 to Evergreen Forest	0.75	3	0
NLCD2011_NALC2010	21043	Shrunken from 21 to Mixed Forest	0.75	3	0
NLCD2011_NALC2010	21052	Shrunken from 21 to Shrub/Scrub	0.75	3	0
NLCD2011_NALC2010	21071	Shrunken from 21 to Grassland/Herbaceous	0.75	3	0
NLCD2011_NALC2010	21081	Shrunken from 21 to Pasture/Hay	0.5	16	0
NLCD2011_NALC2010	21082	Shrunken from 21 to Cultivated Crops	0.2	49	0
NLCD2011_NALC2010	21090	Shrunken from 21 to Woody Wetlands	0.75	3	0
NLCD2011_NALC2010	21095	Shrunken from 21 to Emergent Herbaceous	0.75	3	0
NLCD2011_NALC2010	22011	Shrunken from 22 to Open Water	0	4	0
NLCD2011_NALC2010	22012	Shrunken from 22 to Perennial Ice/Snow	0.75	3	0
NLCD2011_NALC2010	22031	Shrunken from 22 to Barren Land	0.75	3	0
NLCD2011_NALC2010	22041	Shrunken from 22 to Deciduous Forest	0.75	3	0
NLCD2011_NALC2010	22042	Shrunken from 22 to Evergreen Forest	0.75	3	0
NLCD2011_NALC2010	22043	Shrunken from 22 to Mixed Forest	0.75	3	0
NLCD2011_NALC2010	22052	Shrunken from 22 to Shrub/Scrub	0.75	3	0
NLCD2011_NALC2010	22071	Shrunken from 22 to Grassland/Herbaceous	0.75	3	0
NLCD2011_NALC2010	22081	Shrunken from 22 to Pasture/Hay	0.5	16	0
NLCD2011_NALC2010	22082	Shrunken from 22 to Cultivated Crops	0.2	49	0

NLCD2011_NALC2010	22090	Shrunken from 22 to Woody Wetlands	0.75	3	0
NLCD2011_NALC2010	22095	Shrunken from 22 to Emergent Herbaceous	0.75	3	0
NLCD2011_NALC2010	23011	Shrunken from 23 to Open Water	0	4	0
NLCD2011_NALC2010	23012	Shrunken from 23 to Perennial Ice/Snow	0.75	3	0
NLCD2011_NALC2010	23031	Shrunken from 23 to Barren Land	0.75	3	0
NLCD2011_NALC2010	23041	Shrunken from 23 to Deciduous Forest	0.75	3	0
NLCD2011_NALC2010	23042	Shrunken from 23 to Evergreen Forest	0.75	3	0
NLCD2011_NALC2010	23043	Shrunken from 23 to Mixed Forest	0.75	3	0
NLCD2011_NALC2010	23052	Shrunken from 23 to Shrub/Scrub	0.75	3	0
NLCD2011_NALC2010	23071	Shrunken from 23 to Grassland/Herbaceous	0.75	3	0
NLCD2011_NALC2010	23081	Shrunken from 23 to Pasture/Hay	0.5	16	0
NLCD2011_NALC2010	23082	Shrunken from 23 to Cultivated Crops	0.2	49	0
NLCD2011_NALC2010	23090	Shrunken from 23 to Woody Wetlands	0.75	3	0
NLCD2011_NALC2010	23095	Shrunken from 23 to Emergent Herbaceous	0.75	3	0
NLCD2011_NALC2010	24011	Shrunken from 24 to Open Water	0	4	0
NLCD2011_NALC2010	24031	Shrunken from 24 to Barren Land	0.75	3	0
NLCD2011_NALC2010	24041	Shrunken from 24 to Deciduous Forest	0.75	3	0
NLCD2011_NALC2010	24042	Shrunken from 24 to Evergreen Forest	0.75	3	0
NLCD2011_NALC2010	24043	Shrunken from 24 to Mixed Forest	0.75	3	0
NLCD2011_NALC2010	24052	Shrunken from 24 to Shrub/Scrub	0.75	3	0
NLCD2011_NALC2010	24071	Shrunken from 24 to Grassland/Herbaceous	0.75	3	0
NLCD2011_NALC2010	24081	Shrunken from 24 to Pasture/Hay	0.5	16	0
NLCD2011_NALC2010	24082	Shrunken from 24 to Cultivated Crops	0.2	49	0
NLCD2011_NALC2010	24090	Shrunken from 24 to Woody Wetlands	0.75	3	0
NLCD2011_NALC2010	24095	Shrunken from 24 to Emergent Herbaceous	0.75	3	0
BHD_2010	0	Gap 1, 2 or 3 lands	1	1	0
BHD_2010	1	Undeveloped	1	1	0
BHD_2010	2	Residential - rural low (0.001-.0.006 dua)	0.75	1.4	0
BHD_2010	3	Residential - rural (0.006-0.025 dua)	0.5	2.3	0
BHD_2010	4	Residential - exurban low (0.025-0.1 dua)	0.3	6.3	0
BHD_2010	5	Residential - exurban (0.1-0.4 dua)	0.2	16	0
BHD_2010	6	Residential - low (0.4-1.6 dua)	0.1	49	0
BHD_2010	7	Residential - med (1.6-10 dua)	0	256	0
BHD_2010	8	Residential - high (>10 dua)	0	400	0
TIGER_Roads	1100	Interstate	0	400	1
TIGER_Roads	1200	State and local highways, major secondary	0	100	1
TIGER_Roads	1400	City and rural streets	0.75	3	1
TIGER_Roads	1500	Unpaved and AWD	0.75	3	1
TIGER_Roads	1630	Highway interchange ramp	0	400	1
TIGER_Roads	1640	Service Drive	0.75	3	1
TIGER_Roads	1710	Walkway/Pedestrian Trail	0.75	3	1
TIGER_Roads	1720	Stairway	0.75	3	1
TIGER_Roads	1730	Alley	0.75	3	1
TIGER_Roads	1740	Private Road for service vehicles	0.75	3	1
TIGER_Roads	1750	Internal U.S. Census Bureau use	0.75	3	1
TIGER_Roads	1780	Parking Lot Road	0.75	3	1
TIGER_Roads	1820	Bike Path or Trail	0.75	3	1
TIGER_Roads	1830	Bridle Path	0.75	3	1

BLM_CA_Roads	3	Road	0.75	3	1
BLM_MT_Roads	1	Road	0.75	3	1
BLM_NV_Roads_100k	0	Trail	0.75	3	1
BLM_NV_Roads_100k	1	Road	0.75	3	1
BLM_ORWA_Roads	0	Obliterated or decommisioned road	0.9	2	1
BLM_ORWA_Roads	1	Closed road	0.9	2	1
BLM_ORWA_Roads	2	Road	0.75	3	1
Roads_ID_IGDC	0	Water	1	1	1
Roads_ID_IGDC	1	Rails to trails	0.75	3	1
Roads_ID_IGDC	2	Road	0.75	3	1
USFS_Region1_Roads	1	Road	0.75	3	1
USFS_Region4_Roads	1	Road	0.75	3	1
USFSRd_CA	3	Road	0.75	3	1
USFSRd_CA2	1	Road	0.75	3	1
USFSRd_CA2	2	Converted, decommissioned, planned	0.75	2	1
THP_CA_Roads	1	Road	0.75	3	1
THP_CA_Roads	2	Proposed or abandoned road	0.9	2	1
Canada_Roads	10	Highway	0	400	1
Canada_Roads	12	Primary highway	0	400	1
Canada_Roads	13	Secondary highway	0	400	1
Canada_Roads	20	Road	0.75	3	1
Canada_Roads	21	Arterial	0.1	9	1
Canada_Roads	22	Collector	0.2	9	1
Canada_Roads	23	Local	0.75	3	1
Canada_Roads	24	Alley/Lane/Utility	0.75	3	1
Canada_Roads	25	Connector/Ramp	0.2	9	1
Canada_Roads	26	Reserve/Trail	0.75	3	1
Canada_Roads	29	Strata (housing developments)	0.2	9	1
Canada_Roads	80	Bridge/Tunnel	0.75	3	1
Canada_Roads	90	Unknown (mostly logging roads, etc)	0.75	3	1
Rails_TIGER_2013	0	Railroad- active	0	25	0
WindTurbines	1	Wind tower	0	100	0
WindTurbines	90	Inner wind tower buffer (≤ 90m)	0.5	10	0
WindTurbines	180	Outer wind tower buffer (90-180m)	0.75	5	0
Elec_TL_ventyx	102	Transmission line - 100-161 Volts	0.75	9	0
Elec_TL_ventyx	103	Transmission line - 230-300 Volts	0.5	16	0
Elec_TL_ventyx	104	Transmission line - 345 Volts	0.4	25	0
Elec_TL_ventyx	105	Transmission line - 500 Volts	0.4	25	0
Elec_TL_ventyx	106	Transmission line - DC Line	0.4	25	0
Elec_TL_ventyx	107	Transmission line - Step-Up	0.75	9	0
Elec_TL_ventyx	108	Transmission line - Under 100 V	0.75	9	0
NaturalGas_pipeline	1	Natural Gas Pipelines	0.75	9	0
WaterBands	1030	Open Water 0 to 30 m from shore	0	4	0
WaterBands	1060	Open Water 30 to 60 m from shore	0	33	0
WaterBands	1090	Open Water 60 to 90 m from shore	0	66	0
WaterBands	1120	Open Water 90 to 120 m from shore	0	100	0
WaterBands	1150	Open Water 120 to 150 m from shore	0	133	0
WaterBands	1180	Open Water 150 to 180 m from shore	0	166	0

WaterBands	1210	Open Water 180 to 210 m from shore	0	200	0
WaterBands	1240	Open Water 210 to 240 m from shore	0	233	0
WaterBands	1270	Open Water 240 to 270 m from shore	0	266	0
WaterBands	1300	Open Water 270 to 300 m from shore	0	300	0
WaterBands	1330	Open Water 300 to 330 m from shore	0	333	0
WaterBands	1360	Open Water 330 to 360 m from shore	0	366	0
WaterBands	1390	Open Water 360 to 390 m from shore	0	400	0
WaterBands	1420	Open Water 390 to 420 m from shore	0	433	0
WaterBands	1450	Open Water 420 to 450 m from shore	0	466	0
WaterBands	1480	Open Water 450 to 480 m from shore	0	500	0
WaterBands	2000	Open Water > 480 m from shore	0	500	0

Notes: Table adapted from Excel worksheets used to calculate source weight and resistance rasters using Gnarly Landscape Utilities. Expand cells column indicates whether a class was expanded and by how many pixels.

Appendix C: Further Detail on Moving Window Algorithm and Computational Shortcut

In this appendix we further describe the moving window algorithm, particularly the use of the computational shortcut to speed processing.

Scaling flow by target weight or by source and target weights

The moving window algorithm can be run in two ways: either more current can flow to each target when there are more source pixels, or a fixed amount of current can be apportioned among all sources. In the former case, the flow in a landscape (after results from all moving windows are added up) will scale with the square of the amount of natural land. Double the natural land, and you quadruple the flow (and the inferred importance of keeping it connected). In the latter case, flow scales linearly with the amount of natural land (double the amount of natural land, and flow doubles).

The two cases produce similar maps, but the former case (flow scales with the square of natural land) emphasized intact landscapes at the expense of coastal areas and landscapes with any appreciable degree of human use. We felt the latter case, where each target accepts a fixed amount of current regardless of the number of sources, produced more useful maps of connectivity for our primary analyses. The approach still clearly identified intact landscapes (Map 6), but better highlighted more subtle patterns of connectivity in coastal areas and in working landscapes, where there were still valuable natural lands to connect. In other words, scaling flow by natural land rather than the square of natural land meant that the signal from intact landscapes did not overwhelm that of partially developed and coastal landscapes.

By contrast, we used the former case (more current flows to each target when there are more source pixels) for the pilot climate gradient analysis. This was simpler conceptually, because we could scale flow by the number of temperature matches (with a match being defined by a source cell connecting to a target cell that was at least 1 $^{\circ}$C cooler but no more than 5 $^{\circ}$C cooler). However, this is experimental and an argument could still be made for scaling flow by the weight of the target pixels. One could think of this weight as a 'carrying capacity,' with each target pixel having a fixed capacity to receive immigrants. Parameterization decisions such as these must be more fully explored.

Note that because we used different approaches (case 2 and case 1 above, respectively) for our primary and pilot climate analyses, maps 4 and 7 are not directly comparable. They can still be compared qualitatively however.

Computational shortcut

Our moving window method required prohibitive amounts of processing time when the window centered on every pixel in the study area. Each time the moving window centered on a natural or semi-natural pixel required exporting rasters and calling Circuitscape, a relatively time-intensive program, to map current flow within the window. Analyzing our study area in this way could easily have required months of processing time.

To speed up processing, we employed a computational shortcut in which the moving window centered on blocks of pixels rather than on each individual pixel. Pixels in the block with source weights > 0 were considered potential targets for flow, and those in the remainder of the 50-km radius area were considered potential sources (Fig. C1). For each block, we summed the source weights of all potential target pixels, and the target block was assigned a weight equal to this value. A total amount of current equal to this target weight was then allocated to the source pixels in the window in proportion to their individual source weights. This resulted in an amount of current emanating from each source pixel equal to the summed target weights multiplied by the source pixel weight divided by the summed weight of all source pixels. The total flow emanating from all sources was thus equal to the target weight. In this way, the total flow in a landscape scales linearly with the amount of natural lands to connect. As with the simpler case above, the model can alternatively be parameterized such that the total flow is equal to the product of source and target weights, but we found this unreasonably penalized coastal areas and landscapes with any appreciable degree of human use.

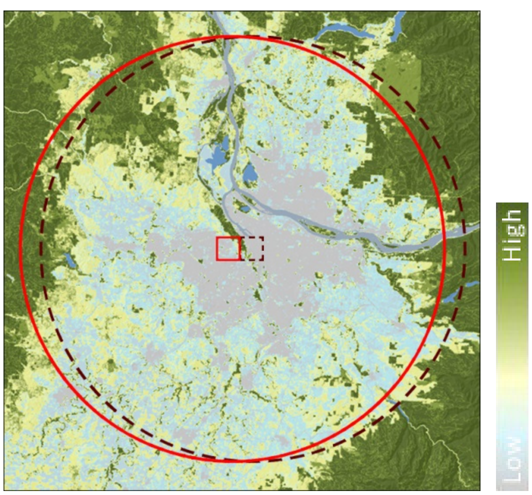

Figure C1. Moving window (solid red circle) centered on a target block of 31 x 31 pixels (solid red square) instead of a single target pixel. All pixels with source weights > 0 inside the window but outside of the center target block are treated as current sources. A single pixel at the center of the target block is set to ground, which acts as the destination for all flow. Total current flow from sources equals the summed source weights of all pixels in the target block. After solving for this moving window, the window would move 31 pixels to the right (dashed dark red circle), and the process would be repeated for the next target block (dashed dark red square).

A single raster with all sources and associated weights surrounding each block and a raster representing a single grounded pixel at the center of the block were then saved to disk. These and a subset of the resistance raster with all cells outside of the radius set to *NoData* were used as inputs to Circuitscape in advanced mode, producing a single current map for the moving window area, as in Fig. 3. After each computation, the window would move to the next block and the process would begin again. Each current map from Circuitscape was multiplied by a correction raster (see below) with the result added into a cumulative current raster.

We experimented with different block sizes, and found that even fairly large block sizes yielded results similar to those without blocking. As reported elsewhere (e.g., McRae et al. 2008), current flow patterns at coarser pixel sizes also approximated those at finer scales. We used a block size of 31 x 31 pixels and a pixel size of 180 m because this struck a reasonable balance between minimizing processing time and reducing artifacts from blocks. Note that flow was not modeled among pixels *within* a block, only between block pixels and the area surrounding the block within 50 km of the block center (Fig. C1). Each pixel with a non-zero source weight was part of a target block once, and was a source for many computations. In several test landscapes, the results closely approximated results achieved with running calculations with the moving window centered on each pixel. Using blocks cut computation time dramatically, replacing as many as 961 (31 x 31) calls to Circuitscape with a single call. This speeded up the algorithm more than 100-fold, without lowering the resolution of the resistance data.

Block analyses still represented approximations of those centered on each pixel, and artifacts were created by the analyses. We employed a simple procedure to remove the artifacts. At the beginning of each run, the OmniScape code calculated the expected current flow pattern using null inputs (a resistance raster with all resistances set to 1, and a source weight raster with all source weights set to 1). From this, we derived the expected current flow pattern to all pixels in a block (in this case adding up 31 x 31 = 961 null current maps, with one map centered on each of the pixels in the block). This formed the null expectation for current flow to the block area under the basic case in which the moving window centered on each pixel. We then calculated the current flow that would be derived with the block code invoked (one calculation with the moving window centered on the block center, and a total of 961 amps injected into pixels outside of the block but inside the 50-km moving window, with the center pixel set to ground). This formed the null expectation for current flow to the block area when the computational shortcut was invoked.

We then divided the null expectation under the case in which the moving window centered on each pixel by the null expectation when the computational shortcut was invoked. This provided a raster that could be used to correct observed current flow for each moving window iteration. Current maps from each iteration were multiplied by the correction raster to remove artifacts before results were summed across all moving windows.